



CryoSat-2 Product Handbook

Baseline D 1.1

C2-LI-ACS-ESL-5319



Table of Contents

1	Introduction.....	7
1.1	<i>Purpose and Scope of this Product Handbook</i>	7
1.1.1	Known issues in the current baseline	7
1.2	<i>Some Basic Altimetry Terms.....</i>	7
1.3	<i>The CryoSat-2 Mission and its Characteristics</i>	9
1.4	<i>Simplified Principles of Operation Modes</i>	10
1.4.1	Low Resolution Mode (LRM)	10
1.4.2	Synthetic Aperture Radar Mode (SAR)	10
1.4.3	SAR Interferometry Mode (SARIn).....	12
1.5	<i>SIRAL Characteristics.....</i>	13
1.6	<i>CryoSat Data Processing</i>	14
1.7	<i>Data Access and Data Processing Tools.....</i>	15
2	Data Parameters and Corrections.....	16
2.1	<i>Spacecraft Orbit and Orientation.....</i>	16
2.1.1	Drifting Orbit and Long Repeat Cycle	16
2.1.2	Orbit processing.....	16
2.1.3	Reference Frame Processing	19
2.2	<i>Spacecraft Time and Location</i>	22
2.2.1	Latitude, Longitude and Altitude	22
2.2.2	DORIS Ultra Stable Oscillator (USO) Drift	22
2.2.3	Reference Ellipsoid.....	22
2.2.4	Geoid and Mean Sea Surface.....	23
2.2.5	Sea Surface Height Anomaly.....	23
2.2.6	Freeboard.....	23
2.2.7	Satellite Velocity Vector.....	23
2.2.8	Reference Orbit.....	23
2.2.9	Ground Tracks.....	24
2.2.10	Illuminated Areas	25
2.3	<i>Instrument Corrections and Noise.....</i>	29
2.3.1	Automatic Gain Control	29
2.3.2	Signal Phase Corrections.....	29
2.3.3	Phase Slope Correction	30
2.3.4	Hamming Weighting Function for SAR Azimuth FFT	30
2.3.5	Noise	34
2.3.6	Echo Saturation.....	35
2.3.7	Doppler Correction	35
2.4	<i>Retracking and Parameters Derived from Echo Shape</i>	35
2.4.1	Range Window and Window Delay	35
2.4.2	Reception Period.....	35
2.4.3	Range Window Sampling	35
2.4.4	Echo Positioning and Scaling	37
2.4.5	Retracking	37
2.4.6	Backscattering.....	38
2.4.7	Peakiness.....	39
2.4.8	Interferometric Mode Specific Parameters	40
2.4.9	Significant Wave Height.....	40
2.4.10	Wind Speed	41
2.4.11	Geophysical Corrections by Surface	41

2.4.12	Surface Type	41
2.5	<i>Range Corrections for Atmospheric Effects</i>	41
2.5.1	Dry and Wet Tropospheric Corrections	42
2.5.2	Ionospheric Correction	42
2.5.3	Inverse Barometric Correction	43
2.5.4	Dynamic Atmospheric Correction.....	43
2.5.5	Sea State Bias	43
2.5.6	Derivation of Corrections.....	43
2.5.7	Application of Corrections to Range.....	43
2.6	<i>Range Corrections for Tidal Effects</i>	43
2.6.1	Ocean Tide	44
2.6.2	Long-Period Equilibrium Ocean Tide	44
2.6.3	Ocean Loading Tide.....	44
2.6.4	Solid Earth Tide	44
2.6.5	Geocentric Polar Tide.....	44
2.6.6	Application of Corrections to Range.....	45
2.6.7	Additional Corrections not applied to Range	45
2.7	<i>Models Used</i>	45
2.7.1	Static Auxiliary Data Files	45
2.7.2	Dynamic Auxiliary Data Files	47
3	CryoSat Data Supply	49
3.1	<i>CryoSat Ground System</i>	49
3.2	<i>CryoSat User Products</i>	49
3.2.1	Level 2 Products and Geophysical Data Record	49
3.2.2	Freeboard Processing	49
3.2.3	Slope Correction	49
3.2.4	Level 1B Products.....	50
3.2.5	Near Real Time Products	50
3.2.6	Fast Delivery Marine Products.....	51
3.3	<i>File Structure</i>	51
3.4	<i>File Naming Convention</i>	51
3.5	<i>Other Conventions</i>	52
3.5.1	Latitude and Longitude Limits	52
3.5.2	Range Correction Sign Convention	52
3.5.3	Timestamp Format.....	52
3.5.4	Time in L2 GDR Records.....	53
4	References and Acronyms.....	54
4.1	<i>Reference Documents</i>	54
4.2	<i>Acronyms and Abbreviations</i>	55

Table of Figures

Figure 1: Basic altimetry terms and applicable corrections over open ocean and sea ice.....	8
Figure 2: Example mode mask.....	10
Figure 3: Geometry of measurement for a single burst.....	11
Figure 4: Geometry of multi-looking.....	11
Figure 5: SARIn mode across-track angle determination.....	12
Figure 6: Cryosat Chronogram.....	14
Figure 7: CryoSat Processors, products and latency.....	15
Figure 8: Example of tracks of CryoSat-2's orbit over a three-day period.....	16
Figure 9: Satellite Reference Frame	20
Figure 10: : Beam-limited footprint.....	26
Figure 11: Variation of the beam-limited footprint with latitude	26
Figure 12: Pulse-limited and Pulse-Doppler limited footprints.....	27
Figure 13: Difference between sampling and Doppler footprint	29
Figure 14: Hamming weighting function	32
Figure 15: Azimuth FFT of a single burst: the nadir clutter is the 'line' in the middle	33
Figure 16: Azimuth FFT of a single burst with hamming: the nadir clutter is reduced.....	33
Figure 17: Stack 60 without hamming: here the parabola is the nadir clutter	34
Figure 18: Stack 60 with hamming: the nadir clutter has disappeared.....	34
Figure 19: Idealised pulse-limited waveform in window	38
Figure 20: Peakiness by latitude	39
Figure 21: Proportion of specular points by latitude	40

Table of Tables

Table 1: Satellite main characteristics..... 9

Table 2: SIRAL characteristics 13

Table 3: Changes between POE-E and POE-F..... 17

Table 4: Retracker used in Baseline-D Ice processor 37

Table 4: Geophysical Corrections applied to Level 2 products over each surface type 41

Table 6: Static auxiliary data files..... 45

Table 7: Dynamic ADFs used in the processing of CryoSat data products 47

Table 8: Relevant File Types..... 52



Document Change Log

Revision	Date	Details of changes
D 1.0	3-APR-2019	Brought up to date for Baseline D.
D 1.1	13-DEC-2019	Integrated updates from IDEAS Performed internal review and integrated comments

This revision of the product handbook is based largely on early work by Catherine Bouzinac and contains contributions from many other people based at ESA, UCL, ACS, ARESYS, Exprivia, and at other locations.

1 Introduction

1.1 Purpose and Scope of this Product Handbook

This document is intended to give CryoSat-2 data users a concise overview of the Level 2 (L2) ice products. This revision of the document has been released to accompany the delivery of the Baseline-D CryoSat ice products. More information about CryoSat product baselines may be found at <https://earth.esa.int/web/guest/missions/CryoSat/ipf-baseline>.

From Baseline-D onwards, the ice products are in a self-describing NetCDF format, and can be read into any program that supports reading NetCDF data. This document is intended to help users understand and use the contents of the products. For a complete list of the contents and structure of the products, see the appropriate Product Format Specification (PFS) documents:

- CryoSat Ice NetCDF L1B Product Format Specification, CS-RS-ACS-ESL-5364[RD 10]
- CryoSat Ice NetCDF L2 Product Format Specification, CS-RS-ACS-ESL-5265[RD 11]

A global attribute in the NetCDF product named `reference_document` gives the specific PFS document ID and revision that applies to that specific product.

1.1.1 Known issues in the current baseline

The following issues have been identified with the current processing baseline at the time of writing.

- Waveforms in the L1b data are represented using the full range of values for their variables. When reading the data into Python, this may cause any bins equal to the maximum possible value to instead be represented as missing data. (`pwr_waveform_20_ku`, `pwr_waveform_avg_01_ku`)
- The SARIn ambiguity flag is never set L2 products, but is correctly set in L2i products. (`flag_prod_status_20_ku`)
- The peakiness value in SAR mode is 0.1 of the correct value over non-ocean surfaces, but is correct over ocean surfaces. (`peakiness_20_ku`)

For an up to date report on the status of the current baseline, see:

<https://earth.esa.int/web/guest/missions/cryosat/product-status>

1.2 Some Basic Altimetry Terms

Basic terms used in the CryoSat-2 mission are :

Range:	the one-way distance from the satellite to the sensed surface below.
Altitude:	the distance from the satellite centre of mass (CoM) to the reference ellipsoid at nadir.
Corrections:	Values to be added to the <i>Range</i> in order to remove effects due to the delay of the echo propagation through the atmosphere, the temporally subsampled high frequency geophysical signals, and the instrumental noise.
Height:	Difference between the <i>Altitude</i> and the corrected <i>Range</i> , i.e. the instantaneous elevation of the surface observed above the reference ellipsoid.
Mean Sea Surface:	Temporal average of the sea <i>Height</i> over a given period which contains both the signature of the marine geoid and of the sea elevation due to the mean oceanic circulation.
Sea Height Anomaly:	Difference between the <i>Height</i> and the <i>Mean Sea Surface</i> corresponding to the variable component of the instantaneous elevation.

Mean Topography: Difference between the *Mean Sea Surface* and the *Geoid*, corresponding to the surface signature of the single mean oceanic circulation.

Absolute Dynamic topography: *Mean Dynamic Topography* plus *Sea Height Anomaly* (or equivalently *Height* minus *Geoid*) containing the surface signature of both the mean circulation and transient oceanographic processes.

Note that most radar altimeters are assumed to observe the first return from the surface at nadir, but CryoSat can observe off-nadir when it operates in SARin mode. If the observation is off-nadir then the latitude and longitude of the actual observed point observed is provided in the data products. LRM products may also contain an off-nadir location where a slope model is available to compute the actual point of first return.

At level 1b, only the engineering corrections (including the USO), the Doppler corrections and the centre-of-mass offset (explained in sections 2.2.2, 2.3.7 and 2.1.3) are applied to the range measurement (given as a time delay `window_del_20_ku`). The altitude is given as `alt_20_ku`.

At level 2, the atmospheric and tidal corrections (explained in sections 2.5 and 2.6) are also applied to the range before it is used to compute height. The heights presented in the L2 products are contained in variables that have the string 'height' in the name, e.g. `height_1_20_ku`.

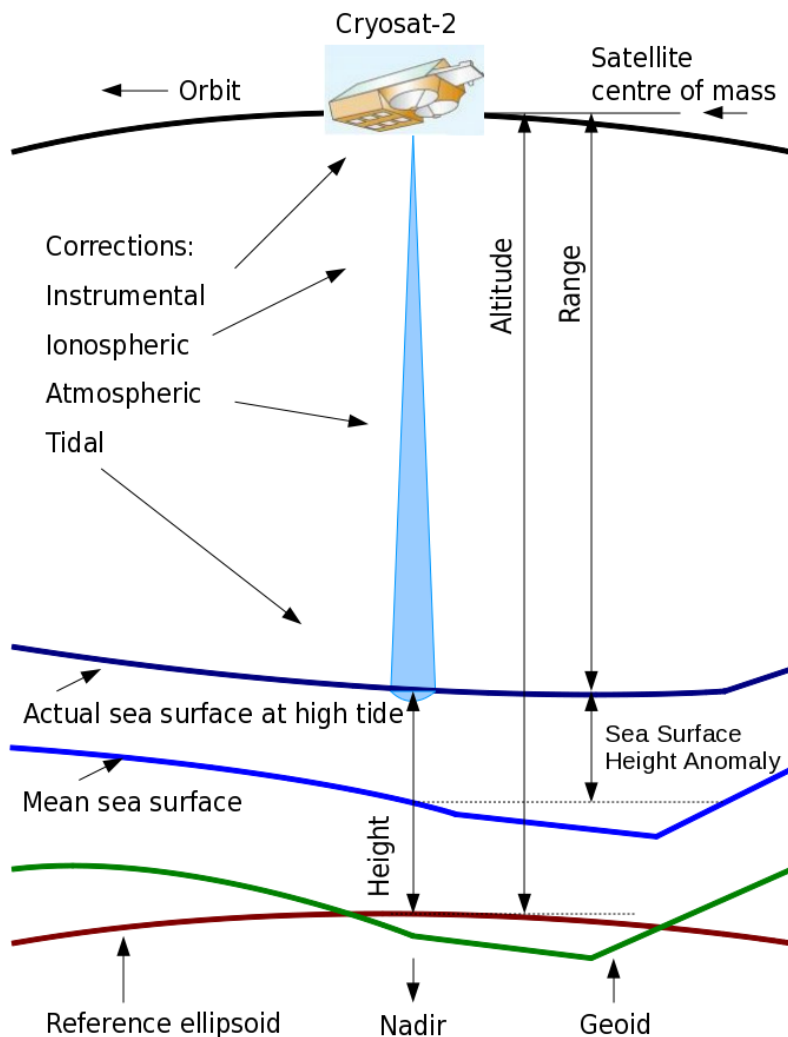


Figure 1: Basic altimetry terms and applicable corrections over open ocean and sea ice

1.3 The CryoSat-2 Mission and its Characteristics

CryoSat-2 is a radar altimetry mission, launched on 8 April 2010, to monitor variations in the thickness of the Earth’s marine ice cover and continental ice sheets. Its primary objective is to measure the extent of thinning Arctic ice due to climate change. However, beyond the core of the mission objective, CryoSat-2 also represents a valuable source of data for the oceanographic community.

The CryoSat-2 satellite replaces the original CryoSat, which was lost due to a launch failure in October 2005. Its main characteristics are summarized in Table 1 below:

Table 1: Satellite main characteristics

Launch	Mission duration	Orbit	Payload	Mass	Dimensions
08 April 2010	Extension until 2019 approved	<ul style="list-style-type: none"> - Low Earth Orbit - Non Sun-synchronous - Altitude: 730 km - Inclination: 92 degree - Repeat cycle: 369 days (5344 orbits) with 30-day sub-cycle 	<ul style="list-style-type: none"> - SAR Interferometric Radar Altimeter (SIRAL) - DORIS receiver - Laser retro-reflector - 3 Star trackers 	720 kg	4.60 m x 2.4 m x 2.2 m

From an altitude of just over 700 km and reaching latitudes of 88°, CryoSat-2 (hereafter CryoSat) monitors precise changes in the thickness of the polar ice sheets and floating sea ice. The observations made over the lifetime of the mission have provided conclusive evidence of rates at which ice cover may be diminishing.

A SAR Interferometric Radar Altimeter (SIRAL) is the primary instrument on-board CryoSat and has extended capabilities to meet the measurement requirements for ice-sheet elevation and sea-ice freeboard. Derived from the well-known Poseidon ocean altimeter on the Jason satellite, SIRAL is a very compact assembly, weighing just 90 kilograms. The SIRAL instrument combines a conventional pulse-limited radar altimeter and a second antenna with synthetic aperture and interferometric signal processing, and is capable of operating in three modes: Low Resolution Mode (LRM) i.e. pulse-limited operation, Synthetic Aperture Radar (SAR) and SAR Interferometric (SARIn or SIN) burst modes. It combines these three measurement modes to determine the global topography, with each mode being optimised for a different surface type:

- Over the **ice sheet interiors** and **oceans**, CryoSat generally operates like a traditional radar altimeter in **Low Resolution Mode (LRM)**.
- Over **sea ice** and **few oceanographic areas**, coherently transmitted echoes are combined via **Synthetic Aperture Radar processing (SAR mode)** to reduce the illuminated surface area. This mode is mainly used to carry out high-resolution measurements of floating sea ice and land ice sheets, enabling the indirect measurement of ice thickness.
- CryoSat's most advanced mode is used around the **ice sheet margins** and over **mountain glaciers**. Here, the altimeter performs **SAR** processing and uses the second antenna as an **interferometer** to determine the across-track angle to the earliest radar returns. This mode (so-called **SIN** or **SARIn** provides the exact surface location being measured when the surface is sloping and (due to an extended range window in this mode) can be used to study

more contrasted terrains, like the very active areas located at the junction of the ice sheet and the Antarctic continent or Greenland.

The measurement modes are operated on-board according to a geographical mode mask. The mask is updated every two weeks to allow for seasonal changes in sea ice extent. The geographical mask is converted into a weekly timeline of instrument commands by the mission planning facility, taking into account the CryoSat reference orbit. An example of the mode mask, downloaded from the ESA website at the URL <https://earth.esa.int/web/guest/-/geographical-mode-mask-7107> is shown in Figure 2. The URL given always points to the latest version. For an archive of older versions, see https://earth.esa.int/web/guest/missions/esa-operational-eo-missions/cryosat/content/-/asset_publisher/VeF6/content/cryosat-mode-mask-archive

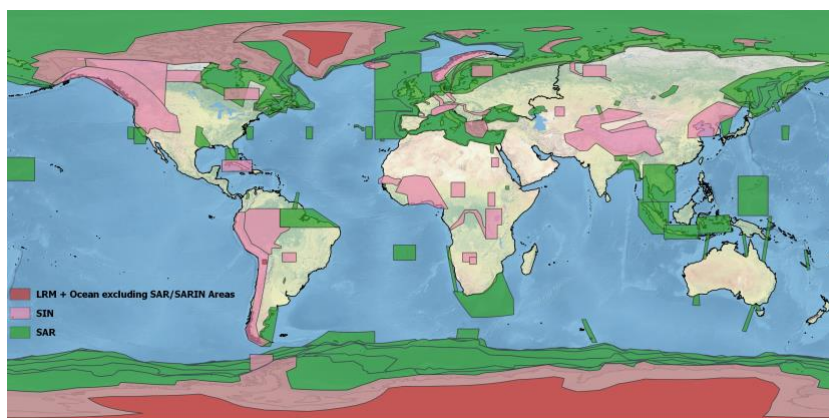


Figure 2: Example mode mask (v4.0 on 13-DEC-2019)

1.4 Simplified Principles of Operation Modes

1.4.1 Low Resolution Mode (LRM)

Conventional radar altimeters operate in pulse-limited mode for which the area of the surface seen by the instrument is limited by the length of the radar pulse transmitted by the altimeter. In CryoSat this mode is referred to as LRM and the data rate is much lower than for the other measurement modes. In pulse-limited mode radar pulses are sent at intervals of about $500\mu\text{s}$ ($\sim 2000\text{Hz}$) ensuring that the returning echoes are uncorrelated. Many uncorrelated echoes can be averaged to reduce speckle. This mode of measurement is suitable over the relatively smooth ice sheet interiors or over open ocean (red on Figure 2, and also where no other mode is shown).

1.4.2 Synthetic Aperture Radar Mode (SAR)

The SAR mode (green in Figure 2) is mainly used over relatively flat areas of sea ice. The CryoSat altimeter sends a burst of pulses with an interval of only $50\mu\text{s}$ ($\sim 20,000\text{Hz}$) partitioning the pulse-limited footprint. Given that the observed surface is in movement relative to the satellite, the echoes received by the radar include a mix of Doppler frequencies corresponding to all surface directions covered by the radar antenna beam, from the front to the back, see Figure 3. In this figure, only 8 beams are shown for clarity (instead of the 64 which are generated) and the divergence angle between them is exaggerated.

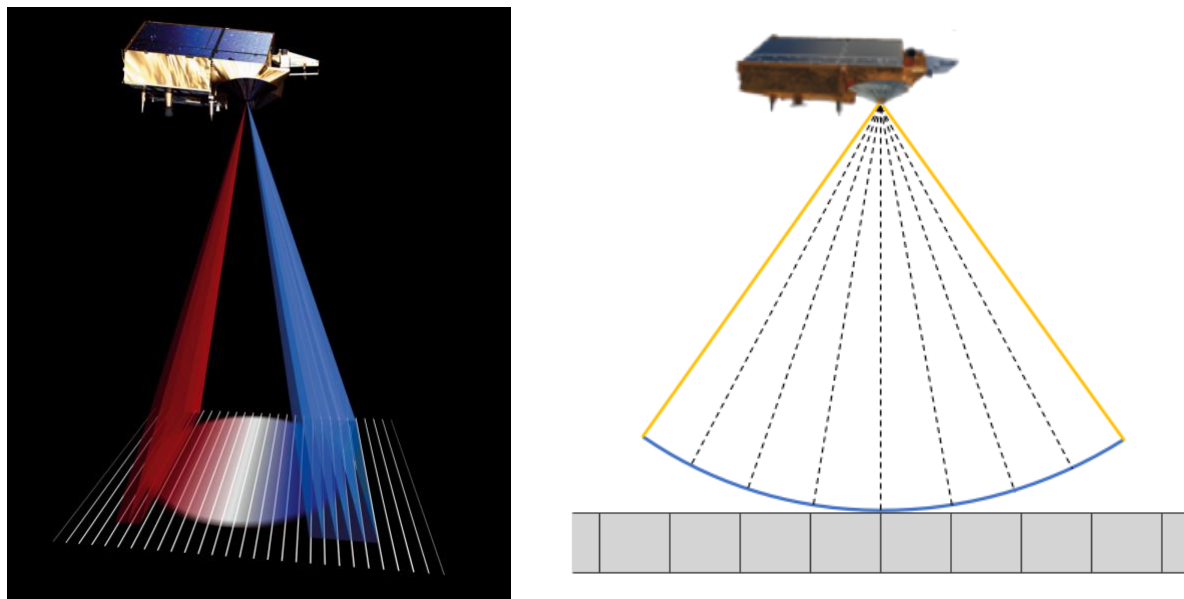


Figure 3: Geometry of measurement for a single burst.

As the returning echoes are correlated, and by treating the whole burst at once, the data processor can separate the echo into 64 strips perpendicular to the track by exploiting the slight frequency shifts caused by the Doppler effect.

Each strip is about 250 m wide and the interval between bursts is arranged so that the satellite moves forward by 80 m each time. Therefore, each ground location is measured multiple times. Figure 4 illustrates this process, where, the blue rectangle is the multi-looked footprint.

The strips measured by successive bursts can therefore be superimposed on each other to create a stack of echoes which are then averaged to reduce noise.

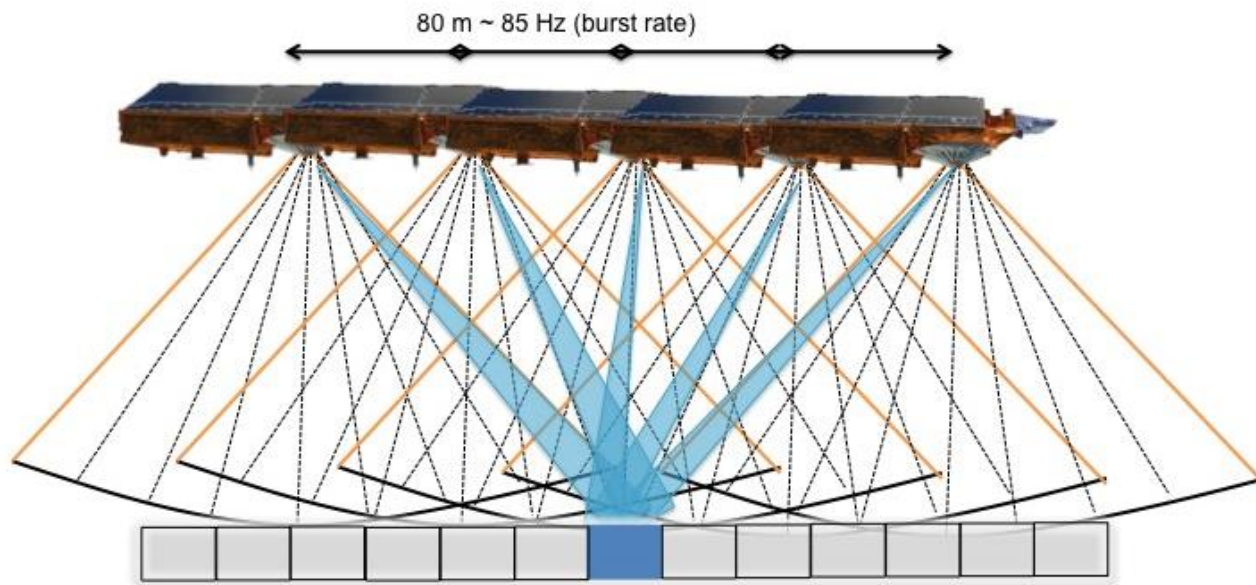


Figure 4: Geometry of multi-look

1.4.3 SAR Interferometry Mode (SARIn)

SAR interferometry (SARIn or SIN), mode (purple in Figure 2) is used across ice sheet margins where the ice surface may be sloping. SIRAL has two antennae, mounted about 1m apart, which receive the echo almost simultaneously. If the echo comes from anywhere but directly below the satellite, then there is a difference in the path lengths of the signal travelling to both antennae. By comparing the difference in signal phases, the angle of arrival and hence the echo origin can be derived. In this mode, the range window is extended to reduce the chance of the echo moving out of the range window (due to changes in topography over the steeply sloping surfaces) before the onboard tracker can reposition the window.

Whilst most radar altimeters have to assume they are observing the surface at nadir, or use a slope model to make the off-nadir correction over sloping surfaces, CryoSat can directly detect when measurements are off-nadir when operating in SIN mode.

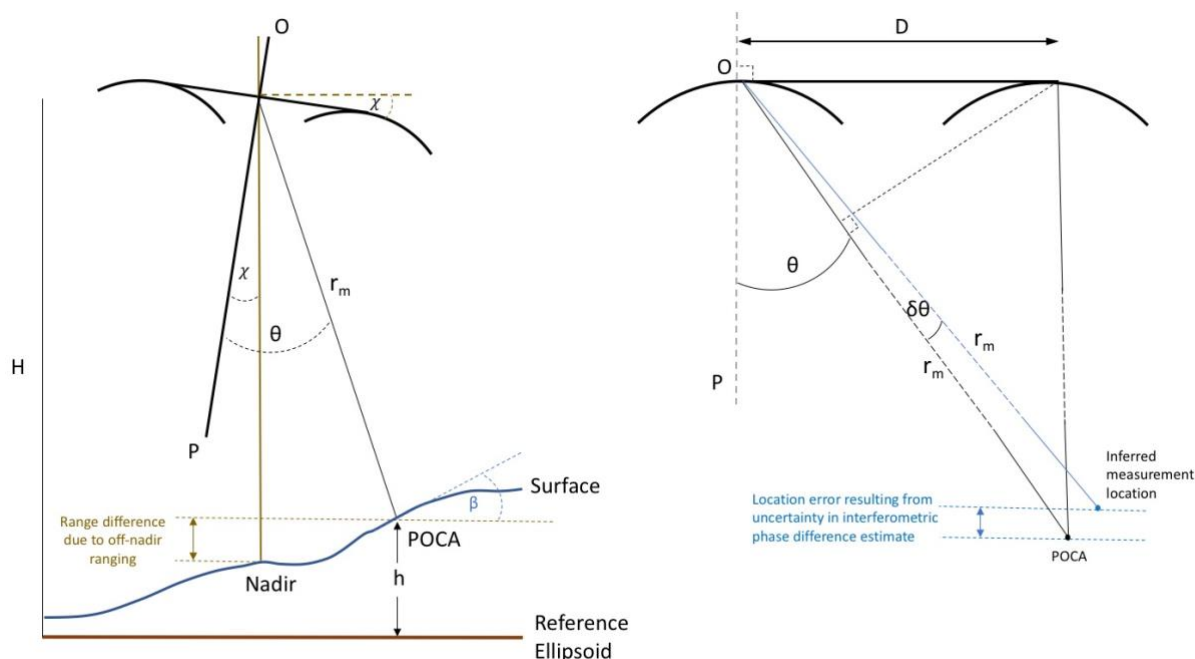


Figure 5: SARIn mode across-track angle determination

The phase difference is used to determine the across track angle :

$$\Delta r \approx D \sin(\theta)$$

$$\text{Surface elevation } h = H - r \cos(\theta)$$

The effect of an error in measuring θ will result in a positive height error δh . The angle error $\delta\theta$ may be due to a combination of spacecraft attitude knowledge errors and instrument measurement errors.

$$\text{Elevation error } \delta h \approx \frac{H(\delta\theta)^2}{2}$$

The error in across track angle has also resulted in an error in the location that the measurement is referenced to (not at the actual point of first reflection). The height error at that location in Figure 5 depends on the shape of the surface at the inferred location. Another way to assess the error would be to consider the height error compared to the height at the point of actual first return, and the horizontal displacement of the inferred measurement location from that point.

If one SIRAL receive chain should fail then the instrument can operate in SIN mode with only one channel. This is referred to as SIN degraded mode, or SID. Instead of the interferometry method, the slope model intended for LRM is used to try to improve the result by estimating the across-track angle. Alongside these operating modes there are specific instrument calibration modes, the pulse response calibration, the receive chain calibration and the interferometric external calibration. Information from these is fed into the higher-level data products and contained in the L1B data products.

Further information is given in reference [RD 1]. An overview of SIRAL is given in [RD 13].

1.5 SIRAL Characteristics

The following table lists the parameters of the SIRAL instrument.

Table 2: SIRAL characteristics

Radio frequency	13.575 GHz (single frequency Ku-band radar)
Pulse bandwidth	320 MHz (40 MHz for tracking only in SIN)
Pulse Repetition Frequency (PRF)	1.97 kHz in LRM, 18.181 kHz in SAR and in SIN; coherent pulse transmission for Doppler processing
Burst Repetition Frequency	N/A in LRM, 85.7 Hz in SAR and 21.4 Hz in SIN
Pulses/burst	N/A in LRM, 64 in SAR and in SIN
Compressed pulse length	3.125 ns
Pulse duration	44.8 μ s
Timing	Regular PRF in LRM, burst mode in SAR and SIN
Samples in echo	128 in LRM; 256 in SAR; 1024 in SIN
RF peak power	25 W
Antenna size	2 reflectors 1.2 m x 1.1 m, side-by-side
Antenna beamwidth (3 dB)	1.06 ^o (along-track) x 1.1992 ^o (across-track)
Antenna footprint	15 km
Range bin sample	0.2342 m for SAR and SIN, 0.4684 m for LRM
Data rate	60 kbit/s for LRM, 12 Mbit/s in SAR, 2 x 12 Mbit/s in SIN
Instrument mass (with antennas)	90 kg redundant
Instrument power	149 W
Tracking cycle	47.17 ms (not a multiple of PRF)
Burst repetition	11.8 ms (not a multiple of PRF)
Antenna baseline length	1167.6 mm

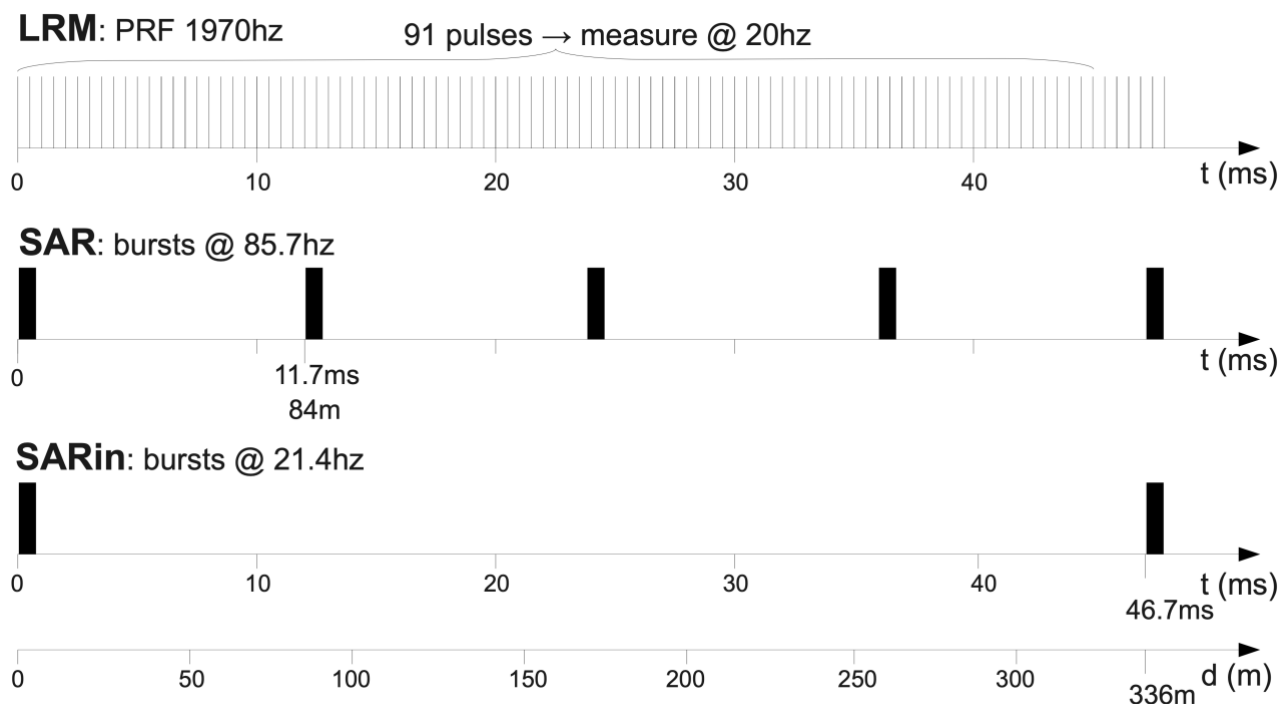


Figure 6: Cryosat Chronogram

For more details, please refer to the ESA webpage at

<https://earth.esa.int/web/eoportal/satellite-missions/c-missions/cryosat-2>

1.6 CryoSat Data Processing

CryoSat Level 0 (L0) data is processed operationally to science L1B and L2 products using two independent processing chains: Ice and Ocean. Both processors generate a range of operational products with increasing latencies and accuracies.

Ice Processor:

- **Near Real Time (NRT) products** – Fast Delivery Marine (FDM) products (LRM) and NRT SAR and SIN mode products, generated within 3 hours of data sensing acquisition using the DORIS Navigator Orbit.
- **Offline products** – LRM, SAR and SIN products typically generated 30 days after data sensing acquisition using consolidated DORIS precise orbits (CNES Precise Orbit Ephemeris).

For more information, see Section 3.2.

Ocean Processor:

- **NRT Ocean Products (NOP)** – LRM, SAR and SIN products generated within 3 hours from data sensing acquisition using the DORIS Navigator Orbit.
- **Intermediate Ocean Products (IOP)** – LRM, SAR and SIN products generated 2-3 days after data sensing acquisition using DORIS preliminary orbits (CNES Medium Orbit Ephemeris).
- **Geophysical Ocean Products (GOP)** - LRM, SAR and SIN products typically generated 30 days after data sensing acquisition using consolidated DORIS precise orbits (CNES Precise Orbit Ephemeris).

For more information about the CryoSat ocean products, please refer to the CryoSat Ocean Product Handbook [RD 27].

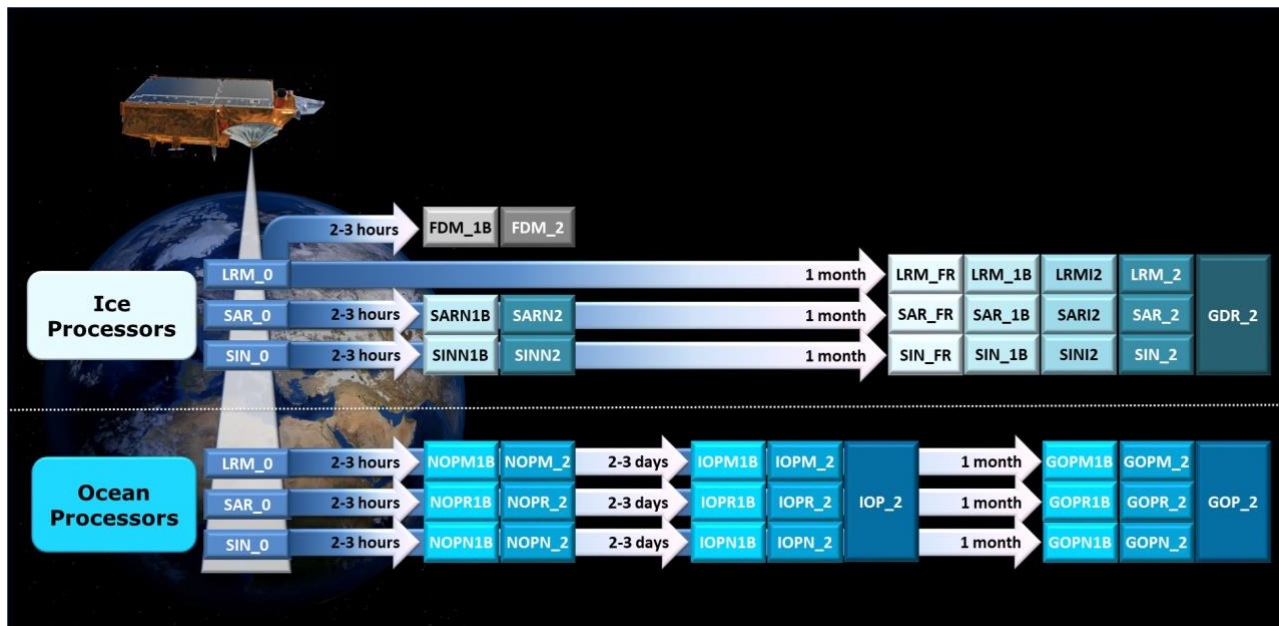


Figure 7: CryoSat Processors, products and latency.

1.7 Data Access and Data Processing Tools

Access to CryoSat data is controlled by a registration system. To register, or to download data if already registered, visit ESA Earthnet Online CryoSat portal at:

<https://earth.esa.int/web/guest/missions/esa-operational-eo-missions/CryoSat>

Another useful website is the ESA radar altimetry tutorial site, which includes links to tools available for data analysis as well as a general discussion of radar altimetry principles:

<http://earth.eo.esa.int/brat/>

Beginning with the Baseline-D Ice processor, CryoSat L1B and L2 products are produced in NetCDF. For older Baselines, which generated products in Earth Explorer (EE) format, a set of API routines are available through the ESA Earthnet Online website in the section ‘Software Routines’. The API libraries have been supplied by UCL and provide ingestion routines written in ANSI C and IDL that can be used to read the L1B and L2 CryoSat products. The download package includes a reference manual and examples.

All CryoSat science products are available on the CryoSat dissemination server (<ftp://science-pds.cryosat.esa.int>). All ‘Offline’ products are processed with the DORIS precise orbits and are generated with a delay of about 30 days after SIRAL acquisition. Near Real Time (NRT) products are generated much sooner after acquisition (see section 3.2.5).

2 Data Parameters and Corrections

Please note that the relevant fields in the data records are referenced by their variable names taken from the Baseline-D NetCDF products and are presented in monospaced font.

2.1 Spacecraft Orbit and Orientation

2.1.1 Drifting Orbit and Long Repeat Cycle

The choice of the CryoSat orbit is the result of trade off between the desired high density of crossover point in order to meet the mission requirements and the need to sufficiently cover southern Greenland. For this, CryoSat's orbit has a mean altitude of 717 km and a high inclination of 92° , allowing measurements at high latitudes (up to 88°). This orbit is non-sun-synchronous and drifts through all angles to the Sun in approximately 16 months. Further information is given in [RD 3]

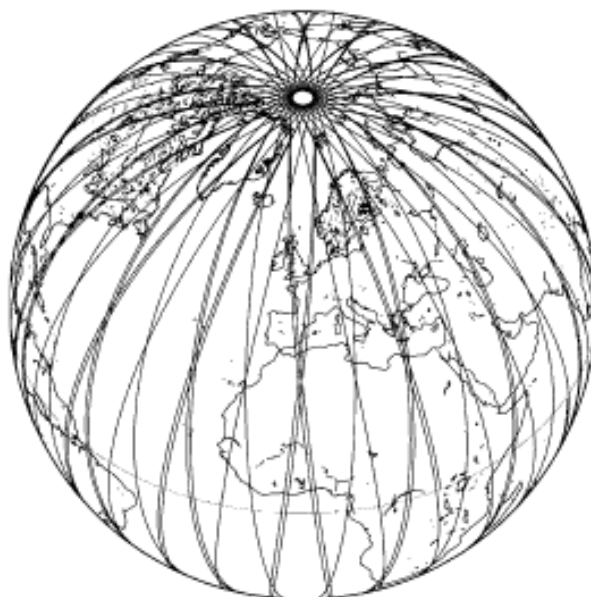


Figure 8: Example of tracks of CryoSat-2's orbit over a three-day period

The repeat cycle for CryoSat orbit should be 369 days, corresponding to 5344 revolutions. **It is however important to note that the CryoSat orbit does not exactly repeat after each cycle**, as it is usually the case for ocean-oriented altimetry missions. CryoSat's ascending nodes are repeating from cycle to cycle within a few tens of meters in order to have equidistant ascending equator crossings in the reference ground track. The descending nodes are however no longer equidistant due to a residual rotation of the eccentricity vector, therefore fluctuations up to nearly 4 km can still be observed on the descending node from cycle to cycle.

2.1.2 Orbit processing

In order to measure accurately, the position of the satellite, CryoSat carries some specific equipment:

- DORIS (Doppler Orbit and Radiopositioning Integration by Satellite) is a tracking system carried by CryoSat to detect and measure the Doppler shift on signals broadcast from a network of over 50 radio beacons around the world. These signals are used for orbit determination, down to millimetre level, and are essential for accurately measuring the

height of the ice surface. The system has been used on previous altimetry missions.

<https://www.aviso.altimetry.fr/en/techniques/doris.html>

- A small laser retro-reflector reflects light back in exactly the direction it came from. A global network of laser tracking stations fire short laser pulses at CryoSat and time the interval before the pulse is reflected back, providing independent reference measurements of the satellite’s position. The International Laser Ranging Service (ILRS) provides tracking from its global network of laser ranging stations to support the mission.

The primary orbit information for data processing is taken from the DORIS Precise Orbit Ephemeris (POE) or the DORIS Navigator Level-0 (L0) Data. Orbit formats are described in [RD 4], [RD 5], [RD 6], and further information on their use is available in [RD 14]

Systematic ‘Offline’ processing relies on the POE, which becomes available to the Payload Data System (PDS) around 30 days after acquisition. Near Real Time (NRT) processing preferably uses the DORIS Navigator L0 data generated on-board the satellite and downlinked to ground during station visibility.

Precise orbital details used during the processing of a given dataset are found in the instrument characterisation data file, and the name of the file used during processing is listed in the NetCDF global attributes of the product file (see [RD 10] and [RD 11] for details).

For Baseline D, the version of the POE used has been updated from POE-E to POE-F. The differences are shown in the following table (Table 3).

Table 3: Changes between POE-E and POE-F

	POE-E	POE-F
Gravity model	EIGEN-GRGS.RL03-v2.MEAN-FIELD Non-tidal TVG: one annual, one semi-annual, one bias and one drift terms for each year up to deg/ord 80; C21/S21 modeled according to IERS2010 conventions Solid Earth tides: from IERS2003 conventions Ocean tides: FES2012 Oceanic/atmospheric gravity: 6hr NCEP pressure fields (70x70) + tides from Biancale-Bode model Pole tide: solid Earth and ocean from IERS2010 conventions Third bodies: Sun, Moon, Venus, Mars and Jupiter	EIGEN-GRGS.RL04-v1.MEAN-FIELD Non-tidal TVG: one annual, one semi-annual, one bias and one drift terms for each year up to deg/ord 90; C21/S21 non modified Unchanged Ocean tides: FES2014 Oceanic/atmospheric gravity: 3hr dealiasing products from GFZ AOD1B RL06 Unchanged Unchanged
Surface forces	Radiation pressure model: calibrated semi-empirical solar radiation pressure model Earth radiation: Knocke-Ries albedo and IR satellite model Atmospheric density model: DTM-13 for Jason satellites, HY-2A, and MSIS-86 for other satellites	Unchanged Unchanged Atmospheric density model: DTM-13 for Jason satellites, HY-2A, and MSIS-00 for other satellites

	POE-E	POE-F
Estimated dynamical parameters	Stochastic solutions	Unchanged
Satellite reference	Mass and center of gravity: post-launch values + variations generated by Control Center Attitude model: For Jason satellites: quaternions and solar panel orientation from control center, completed by nominal yaw steering law when necessary Other satellites: nominal attitude law	Unchanged Refined nominal attitude laws
Displacement of reference points	Earth tides: IERS2003 conventions Ocean loading: FES2012 Pole tide: solid earth pole tides and ocean pole tides (Desai, 2002), cubic+linear mean pole model from IERS2010 S1-S2 atmospheric pressure loading, implementation of Ray & Ponte (2003) by van Dam Reference GPS constellation: JPL solution - fully consistent with IGS08	Unchanged Ocean loading: FES2014 Pole tide: solid earth pole tides and ocean pole tides (Desai, 2002), new linear mean pole model Unchanged Reference GPS constellation: GRG solution - fully consistent with IGS14
Geocenter variations	Tidal: ocean loading and S1-S2 atmospheric pressure loading Non-tidal: seasonal model from J. Ries, applied to DORIS/SLR stations	Unchanged Non-tidal: full non-tidal model (semi-annual, annual, inter-annual) derived from DORIS data and the OSTM/Jason-2 satellite, applied to DORIS/SLR stations and GPS satellites
Terrestrial Reference Frame	Extended ITRF2008 (SLRF/ITRF2008, DPOD2008, IGS08)	Extended ITRF2014 (SLRF/ITRF2014, DPOD2014, IGS14)
Earth orientation	Consistent with IERS2010 conventions and ITRF2008	Consistent with IERS2010 conventions and ITRF2014
Propagations delays	SLR troposphere correction: Mendes-Pavlis SLR range correction: constant 5.0 cm range correction for Envisat, elevation dependent range correction for Jason DORIS troposphere correction: GPT/GMF model DORIS beacons phase center correction GPS PCO/PCV (emitter and receiver) consistent with constellation orbits and clocks (IGS08 ANTEX), pre-launch GPS receiver phase map GPS: phase wind-up correction	Unchanged SLR range correction: geometrical models for all satellites DORIS troposphere correction: GPT2/VMF1 model Unchanged GPS PCO/PCV (emitter and receiver) consistent with constellation orbits and clocks (IGS14 ANTEX), in-flight adjusted GPS receiver phase map Unchanged

	POE-E	POE-F
Estimated measurement parameters	DORIS: one frequency bias per pass, one troposphere zenith bias per pass SLR: Reference used to evaluate orbit precision and stability GPS: floating ambiguity per pass, receiver clock adjusted per epoch	DORIS: one frequency bias and drift (for "SAA stations") per pass, one troposphere zenith bias per pass, horizontal tropospheric gradients per arc Unchanged GPS: fixed ambiguity (when possible) per pass, receiver clock adjusted per epoch
Tracking Data corrections	Jason-1 Doris data: updated South Atlantic Anomaly model (J.-M. Lemoine et al.) applied before and after DORIS instrument change DORIS time-tagging bias for Envisat and Jason aligned with SLR before and after instrument change	Unchanged Unchanged
Doris Weight	1.5 mm/s (1.5 cm over 10 sec) For Jason-1, SAA DORIS beacons weight is divided by 10 before DORIS instrument change	Process data down to as low elevation angles as possible (from 10° to 5° elevation cut-off angle) with a consistent down-weighting law Unchanged
SLR Weight	15 cm Reference used to evaluate orbit precision and stability	Unchanged
GPS Weight	2 cm (phase) / 2 m (code)	Unchanged

2.1.3 Reference Frame Processing

Knowledge of the precise orientation of the baseline and the two receiving antennas is essential for the success of the mission. CryoSat measures this baseline orientation using the position of the stars in the sky. Three star-trackers are mounted on the support structure for the antennas. Each contains a camera, which take up to five pictures per second. The images are analysed by a built-in computer and compared to a catalogue of star positions.

The CryoSat spacecraft flies in a nose-down attitude inclined at 6 degrees to the positive X axis, see Figure 9. The nadir direction is inclined 6 degrees from the negative Z axis. The origin of the satellite reference frame is at the centre of the satellite mounting plane on the launch vehicle. The radar antennas are mounted such that the real beam direction is along the nadir direction.

Full details are given in [RD 7].

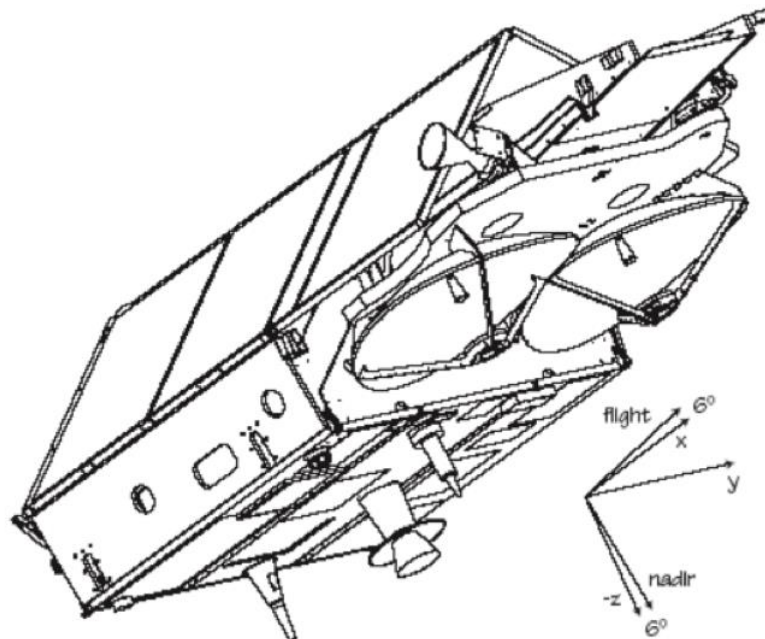


Figure 9: Satellite Reference Frame

This illustration comes from [RD 7] and shows CryoSat, without its thermal control material. Note that the negative Z axis is shown in order to display the offset to the nadir direction.

L1B and L2 products use a CryoSat processing reference frame (not the satellite reference frame) to describe the interferometric antenna baseline (*inter_base_vec_20_ku*) and real antenna boresight (real beam) direction vectors (*beam_dir_vec_20_ku*). This reference frame has its origin at the satellite centre of mass (CoM). In the satellite reference frame, this point is (1.6312, 0.0112, 0.0137). CryoSat has been designed so that the CoM corresponds to the centre of the single, spherical fuel tank. The fuel is gaseous nitrogen, which uniformly fills the tank. CryoSat has no moving parts, consequently the centre of mass will not move during the satellite lifetime. Mass change and any movement is tracked at <ftp://ftp.ids-doris.org/pub/ids/satellites/cs2mass.txt> and there is zero movement at the time of writing. Overall design concerns are given in [RD 3].

The X axis is directed from the frame origin and is parallel with the normal incidence to the reference ellipsoid. The Y axis is in the plane defined by the X axis and the spacecraft velocity vector V. It is determined by

$$Y = (V - X(X \cdot V)) / |V - X(X \cdot V)| \tag{Equation 2.1}$$

The remaining axis is determined by $Z = Y \times X$ (Equation 2.2)

All reference frames used during processing are described in detail in [RD 18].

In other words, the antenna baseline and real beam vectors are defined in the CryoSat processing reference frame (CoM, X, Y, Z) orthonormal but left-handed, where X is the unit vector pointing to nadir in the ‘along-track’ plane defined by the CoG and the velocity vector, and Y is the unit vector almost in the same direction as the velocity vector.

The interferometric baseline vector and the real beam vector components are normalised to make a unit vector and scaled by one million to get integer components in micrometres. These components

are measured by the star tracker angles on board. In the perfect situation, the baseline vector is $[0;0;-1000000]$ and the beam vector is $[1000000;0;0]$.

Since one vector element is nominally one unit and the angles are very small, the roll, pitch, and yaw angles of the antenna bench in the CryoSat processing reference frame can be approximated with :

roll = + (baseline_vector_x) in microradians, where roll is relative to axis Y defined above.

yaw = - (baseline_vector_y) in microradians, where yaw is relative to axis X defined above.

pitch = - (beam_vector_y) in microradians, where pitch is relative to axis Z defined above.

These angles are presented in the following variables at resolutions of 0.1 microdegrees and with all applicable corrections and biases applied:

off_nadir_roll_angle_str_20_ku

off_nadir_pitch_angle_str_20_ku

off_nadir_yaw_angle_str_20_ku

Positive/negative roll corresponds to right antenna down/up respectively.

Positive/negative yaw corresponds to spacecraft nose moving to the right/left respectively.

Positive/negative pitch corresponds to spacecraft nose down/up respectively.

In order to look at the Earth, the satellite turns one revolution in inertial space for each revolution that it makes around the Earth. Since a revolution around the Earth takes roughly 6000 seconds, the rotation rate is about 360 degrees / 6000 seconds, or about 0.06 degrees per second. It is mainly the pitch which must turn in inertial space to follow the Earth. Therefore, if there is a timing error in the datation or a calculation error, one can expect pitch, in particular, to be affected. The impact will be of the order 0.06 degrees/sec multiplied by the delta time.

The SIN phase difference waveforms in L1B data (ph_diff_waveform_20_ku) **do include** a phase difference bias (instr_ext_ph_cor_20_ku), which accounts for the roll fixed bias component only, but **do not include** the roll variable component, which can be extracted in the product itself according to the above formula and should be used, as shown below, to correct the inferred angle.

The variable roll (off_nadir_roll_angle_str_20_ku) can be applied to the inferred angle as a variable correction. The inferred angle alpha is obtained from the retracked SIN L1B phase difference waveform ph_diff_waveform_20_ku with: α [rad] = $\lambda * \text{retrack_PD} / (2 * \pi * \text{baseline})$, where retrack_PD is the retracked phase difference in radians, baseline = 1.1676 m and $\lambda = 0.022084$ m

Then the variable roll correction can be applied to the inferred angle with $\alpha - \text{roll}$. This is computed and applied in the L2 SARIn processing.

Note that the phase difference values (ph_diff_waveform_20_ku) are provided between $-\pi$ and $+\pi$ microradians. A positive/negative phase difference (and across-track inferred angle) corresponds to a signal coming from the right/left hand side of the observer sitting on the antenna bench with their spine aligned with the nadir direction and looking forward in the along-track flight direction.

The mispointing angle is the angle between the antenna pointing, i.e. the direction of the actual beam, and the nadir direction. Nominally this should be zero degrees, but in practice it varies around the orbit by 0.1–0.2 degrees.

2.2 Spacecraft Time and Location

2.2.1 Latitude, Longitude and Altitude

Latitude, longitude and altitude fields are each provided multiple times within the L1B and L2 ice products.

At L1B the 20 Hz latitude (`lat_20_ku`), longitude (`lon_20_ku`) and altitude (`alt_20_ku`) measurements are those interpolated from the orbit at the exact time recorded in the timestamp. Measurements are provided for each 20 Hz measurement (20 measurements per record). All of them are located relative to the reference ellipsoid at nadir to the satellite centre of gravity.

The 1 Hz latitude (`lat_avg_01`), longitude (`lon_avg_01`) and altitude (`alt_avg_01`) of the 1 Hz averaged waveform measurements are provided once per record and give the latitude, longitude and altitude of the orbit corresponding to the nadir position at the time of the 1 Hz average timestamp (`time_avg_01_ku`).

At L2 the 20 Hz fields are only provided for latitude (`lat_poca_20_ku`) and longitude (`lon_poca_20_ku`). In LRM mode these are set to the nadir location unless a corrected location has been computed via use of a slope model. In SAR mode, these locations are at nadir. In SARIn mode, these measurements provide the estimated position of the point of closest approach as computed from the phase difference.

At L2 the 1 Hz latitude (`lat_01`), longitude (`lon_01`) and altitude (`alt_01`) are provided once per record at the time of the 1 Hz correction timestamp (`time_cor_01`).

2.2.2 DORIS Ultra Stable Oscillator (USO) Drift

The DORIS USO drift is required to accurately convert the SIRAL altimeter time and range counts into UTC time tag and range delay measurements. SIRAL derives all its radar frequencies from the DORIS USO whose frequency, in terms of deviations from nominal value (one measurement every 24 hours), is made available in a DORIS L1B product, which is an incremental file. This is described in [RD 5]. The USO correction is provided at 20 Hz (`uso_cor_20_ku`). The average 1 Hz USO correction (`uso_cor_avg_01`) refers to the L1B 1 Hz average power waveform.

The USO correction is applied to the window delay at L1B. The correction applied is given in terms of range at L2 (`uso_cor_applied_20_ku`).

2.2.3 Reference Ellipsoid

Satellite altimeter height measurements are usually referenced to an ellipsoid, a simple mathematical figure that describes a rough approximation of the geoid. The geoid is the shape the sea surface would have under the single influence of Earth's gravitation and without any signatures from the ocean circulation and tide effects. For CryoSat, the reference ellipsoid is WGS84, defined by the National Geospatial Intelligence Agency of the USA. This can be explored online at

<https://www1.nga.mil/ProductsServices/GeodesyandGeophysics/Worldgeodeticsystem/Pages/default.aspx>

2.2.4 Geoid and Mean Sea Surface

In the L2 data product, values of the geoid are provided over land and continental ice, while values of the mean sea surface (MSS) are provided over open ocean and closed seas. In both cases these measurements are spatially interpolated at the ground track locations. The geoid model used is EGM96 `geoid_01` and the MSS model used is UCL13 (`mean_sea_surf_sea_ice_01`).

EGM96 can be explored more fully at <http://cddis.nasa.gov/926/egm96/egm96.html>.

UCL13 is a hybrid global model compiled from CryoSat sea surface height measurements above 60 degrees North and the CLS2011 MSS (<http://www.aviso.oceanobs.com/index.php?id=1615>) below 50 degrees North. Between those two latitudes, a linear blend is performed between the two models. The purpose of the model is to provide better accuracy for sea ice freeboard determination in the Arctic Ocean. Model details are also given in section 2.7.1 and [RD 7]/[RD 26].

2.2.5 Sea Surface Height Anomaly

Sea surface height anomaly (SSHA) is the difference between the long-term average sea surface height, i.e. the MSS, and the ocean height actually observed by the satellite. This must be determined in order to accurately calculate the sea ice freeboard. At level 2, the SSHA is found by comparing the ocean height with the UCL13 MSS to get the ocean height anomaly `ssha_20_ku`, and then using linear interpolation to get the SSHA `ssha_interp_20_ku`. The SSHA quality flag gives the RMS of the residuals of the linear fit `ssha_interp_rms_20_ku`. Technically another MSS may be chosen if desired, as the choice is configurable. Model details are also given in section 2.7.1 and [RD 7] / [RD 26].

2.2.6 Freeboard

Sea ice freeboard (`freeboard_20_ku`) is the height by which an ice floe extends above the sea surface. L2 data includes climatological snow depth (`snow_depth_01`) and density values (`snow_density_01`) for each record. The snow depth values are extracted from a static climatology model UCL04. There is a separate climatology file for each month of the year, which provides snow depth values for the Arctic region only. No climate model for the Antarctic region is available for CryoSat processing. The snow density is currently a constant value (400 kg/ m³) extracted from the Parameter Configuration File (PCONF). Additional model details are also given in section 2.7.1 and [RD 7] / [RD 26].

In Baseline D (and earlier versions), these corrections are provided but not applied to the freeboard. These can be applied by the user to adjust the freeboard estimate to account for snow loading. Please note that the freeboard can possibly be negative where there is heavy snow loading on thin ice.

2.2.7 Satellite Velocity Vector

The satellite velocity vector is provided at L2I (`sat_vel_vec_20_ku`) and is given in the International Terrestrial Reference Frame (ITRF), which is defined and maintained by the International Earth Rotation Service (IERS). For more information: <http://www.iers.org/IERS/EN/Science/science.html>

2.2.8 Reference Orbit

The CryoSat Reference Orbit File includes two phases:

- **Phase 1:** from launch in April 2010 to June 2010. During this 'Commissioning Phase' the CryoSat cycle was not consistent due to continuous orbital manoeuvres which were performed in order to obtain a stable orbit.
- **Phase 2:** from July 2010 onwards. During this phase a stable orbit was maintained.

Please note that data acquired between launch and July 2010 will not be reprocessed, after it was decided that this early data were of little scientific use due to the orbit 24anoeuvres.

2.2.9 Ground Tracks

This section explains the retrieval and analysis of CryoSat orbits and ground tracks files, in order to understand the differences in the ground tracks when using different predictions of the orbit. Information and description about the available files can be found on the ESA CryoSat web page <https://earth.esa.int/web/guest/-/ground-tracks-7209>. The following CryoSat orbit files are provided to CryoSat users:

- The **Reference Orbit** file contains information on the orbits over a full repetition cycle (369 days), generated at the start of every orbital repetition cycle.
- The **Reference Ground Track** file is generated from the Reference Orbit file. Measurements are expressed in latitude and longitude with 2 seconds, 10 seconds or 60 seconds sampling intervals.
- The **Predicted Orbit** file is a high accuracy orbit prediction, generated closer to the time of the overpass. It is generated every day, and contains one Orbit State Vector (OSV) per orbit, located at (or very near to) the ascending node. The coverage is for 30 days starting from the generation time.

As a result, the orbits for a given day can be evaluated from the Reference Orbit file or from 30 different Predicted Orbit files which all contain that day, but with increasingly accurate predictions.

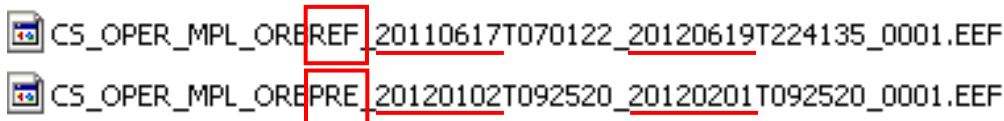
The files mentioned above, and the software to generate them can be retrieved from the FTP server:

FTP server: <ftp://calval-pds.cryosat.esa.int> Username: ground Password: tracks

The FTP server contents following, the following data structure can be observed:

- Reference Orbit files, one per year (2010 onwards)
- Predicted Orbit files, sorted by year, then month, then 1 file per day of that month
- Ground Tracks, available on a monthly or yearly basis and with three different sampling steps (2, 10 or 60 seconds)
- Software folder, which contains the necessary tools to generate ground tracks from the orbit files and other functionalities.

The Ground Tracks files are simple .txt files. Each monthly file contains all the reference ground tracks from that month sampled every 10 seconds. In order to compare the Reference Orbits and Predicted Orbits (example for 2012), the following files can be retrieved from the FTP server:



CS_OPER_MPL_ORBREF_20110617T070122_20120619T224135_0001.EEF
 CS_OPER_MPL_ORBPRE_20120102T092520_20120201T092520_0001.EEF

In this example, the Reference Orbits span from 17 June 2011 to 19 June 2012, whilst the Predicted Orbits span from 02 January 2012 to 01 February 2012.

The time sampling of the Reference Orbit file is 100 minutes, therefore only one OSV is given for each orbit (100 minutes is approximately the orbit period) for the local ascending node. The orbit files content is fully described in the CryoSat Ground System Mission Files Format Specifications [RD 15](pages 9-27). The files contain the time, orbit number and state vector. The X, Y and Z coordinates can be used to calculate the orbit height: $H = (X^2 + Y^2 + Z^2)^{1/2} - R_{equator}$

When comparing the reference and the predicted orbits, the differences in X, Y and Z coordinates are always < 5%.

All the information to calculate the ground tracks from the orbit files is in the pdf documents at:

<https://eop-cfi.esa.int/index.php/applications/tools/command-line-tools-transponder-pass>

Starting with a Reference Orbit or Predicted Orbit file, the executable function returns the ground track points (at a temporal sampling defined in Time Step) which are contained in the area defined in Zone Database, for a given set of orbits or for a given time interval.

The ground track samples retrieved from the oldest predicted orbit (one month before) and the ground track samples retrieved from the newest predicted orbit (one day before) can be slightly different. This difference mainly depends on the time or distance from the last orbit manoeuvre. The spatial difference between the tracks cannot be calculated as simply the distance between two samples of the different ground tracks, because there is a time delay which in turn produces a spatial shift. However, the across-track distance can be easily calculated with some geometry. Nominally, the across-track distance never exceeds 1 km and rarely exceeds 500 m in polar areas.

2.2.10 Illuminated Areas

2.2.10.1 Beam-limited footprint

The beam-limited illuminated area (or ‘footprint’) is defined as the whole area on the Earth’s surface from which a beam echo is collected. It depends mainly on the antenna illumination pattern, and therefore does not vary with the acquisition mode. It can be described by its dimensions in the along-track direction and in the across-track direction, which depend on the antenna pattern. Where ϑ is the antenna beam width at -3 dB, θ_B is the angle of the central beam direction with respect to the nadir, and h is the altitude of the satellite, the width of the beam-limited footprint is calculated by $D = h \cdot \tan(\theta_B + \vartheta/2) - h \cdot \tan(\theta_B - \vartheta/2)$ where the flat Earth approximation is used.

Considering an altitude of 730 km, $\vartheta = 1.06$ degrees and $\theta_B = 0$ degrees along track, while $\vartheta = 1.1992$ degrees and $\theta_B = 0$ degrees across track, the footprint area for SIRAL can be decomposed in:

- width of the beam-limited area along track approximately equal to 13.5 km
- width of the beam-limited area across track approximately equal to 15.3 km

Both the along-track and across-track beam-limited areas are not constant but are dependent on the orbit characteristics and therefore they change with latitude. The width of the beam-limited area along track varies between 13.2 and 14.0 km while the beam-limited area across track varies between 14.9 and 15.8 km.

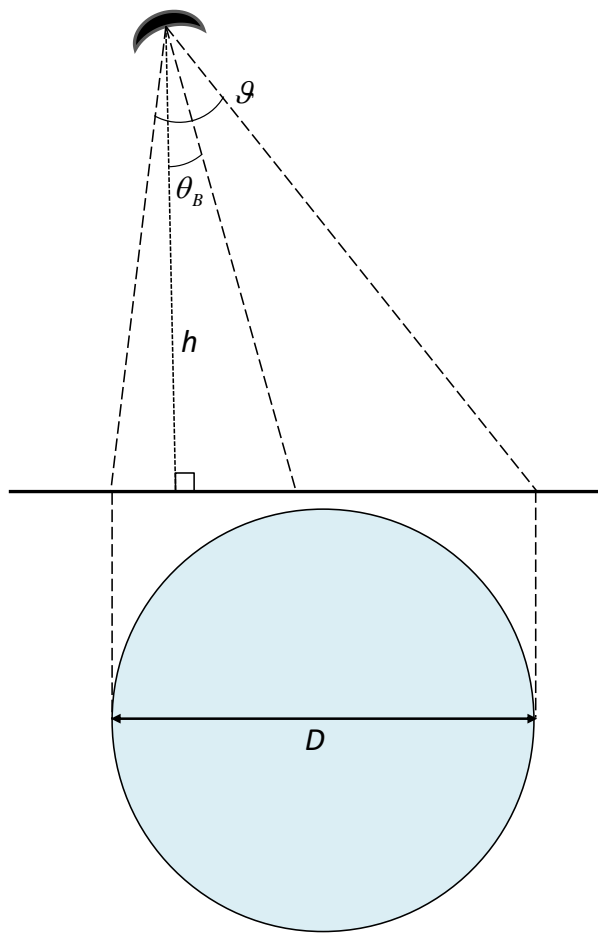


Figure 10: : Beam-limited footprint

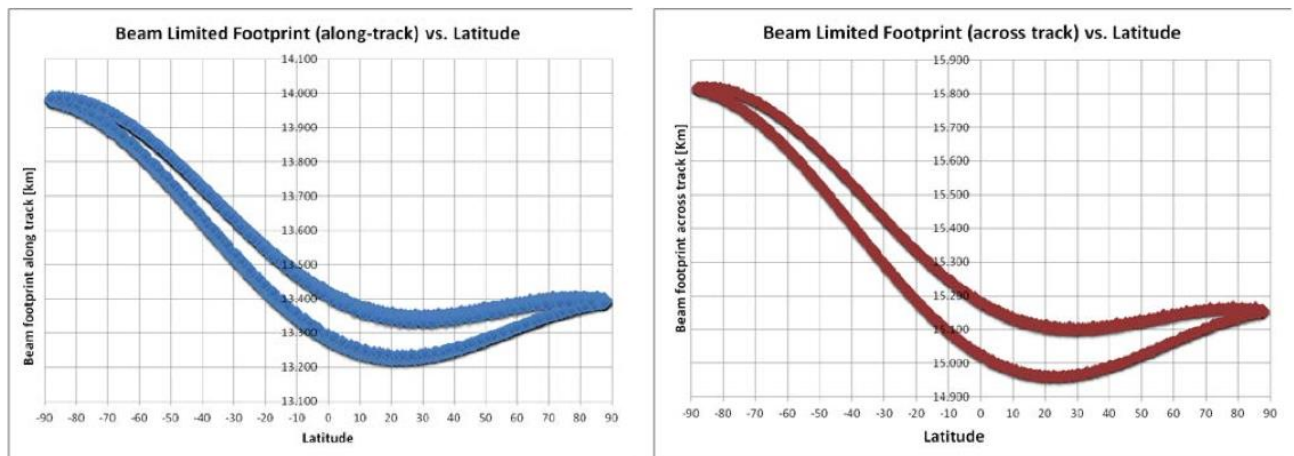


Figure 11: Variation of the beam-limited footprint with latitude

2.2.10.2 Pulse-limited footprint

The pulse-limited footprint is defined as the illuminated area on ground around the point of closest approach and corresponds to the area illuminated by the leading edge of the pulse until the time the trailing edge first intersects the surface. See figure 10.

For LRM, the pulse-limited footprint depends only on the compressed pulse duration, since LRM acquisition has only one independent variable (the time delay).

The Doppler beam formation in SAR and SIN modes are used to discriminate the direction of arrival of the echoes in the along-track direction, so that a pulse-Doppler footprint can be defined. This is facilitated by the inclusion of 2 independent variables in SAR and SIN modes, the along-track position and the across-track position, both related to the time delay.

The width of the footprint for LRM and SAR/SIN modes is defined below using the flat Earth approximation and assuming a quasi-flat ground surface.

2.2.10.3 Pulse-limited footprint for LRM

In conventional altimeter acquisition, such as LRM, the area around the point of closest approach is fully illuminated when the trailing edge of the pulse reaches the Earth’s surface. The pulse-limited footprint can therefore be approximated as a circular area with radius equal to:

$$r = \sqrt{h \cdot c \cdot \tau} = \sqrt{h \cdot \frac{c}{B}}$$

where c denotes the speed of light, h is the altitude of the satellite (730 km) and the compressed pulse length is $\tau = 1/B$ where B is the pulse bandwidth (320 MHz⁻¹).

For SIRAL, the pulse-limited footprint is about 2.15 km², with a width of approximately 1.65 km. It has the same width in both the along-track and the across-track directions since in LRM there is only one independent variable, that is the time delay.

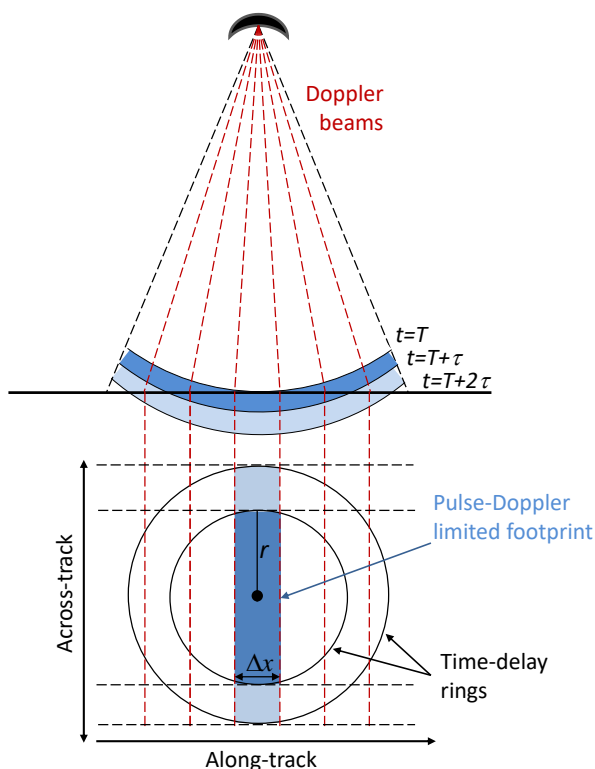


Figure 12: Pulse-limited and Pulse-Doppler limited footprints

2.2.10.4 Pulse-Doppler-limited footprint for SAR and SIN modes

In SAR/SIN acquisition modes, the processor allows the area of the pulse in the along-track direction to be sharpened. As stated before, the Doppler beam formation in SAR/SIN mode allows us to discriminate the direction of arrival of the echoes in the along-track direction as well as to measure the time delay. This way the footprint width is defined independently in the along-track and the across-track directions.

In the across-track direction, the footprint width for SIRAL is defined by the pulse-limited width as in LRM. However, in the along-track direction, the footprint width for SIRAL is defined as the sharpened beam-limited area. The pulse-Doppler-limited area for SAR/SIN can be approximated by a rectangle given by the pulse-limited area width across-track and by the sharpened beam-limited area width along-track. The resolution is determined by the L0 to L1B processing chains.

Since the band of Doppler frequencies that is unambiguously sampled by the Pulse Repetition Frequency (PRF) goes from $-PRF/2$ to $+PRF/2$, and there are 64 different sharpened beams equally spaced in the Doppler domain, the width of the sharpened beam-limited area is:

$$\Delta x = h \frac{\lambda}{2v} \frac{PRF}{64}$$

where h is the altitude of the satellite, λ is the wavelength, v is the velocity of the spacecraft and PRF is the Pulse Repetition Frequency.

For CryoSat, the pulse-limited footprint in the across track direction is approximately equal to 1.65 km while the sharpened beam-limited footprint width in the along-track direction is approximately equal to 305 m, which in turn corresponds to an along-track resolution of approximately equal to 401 m (after weighting), using flat Earth approximation. Hence, the pulse-Doppler-limited footprint for SAR/SIN is about 0.5 km².

The along-track sampling resolution in SAR and SIN modes is variable around the orbit. It is, for example, 278 m based on an altitude of 750 km, flat Earth and half power of the azimuth beam. This is then affected by the azimuth hamming weighting function which degrades the resolution. The sampling of the processor is different to the resolution (see Figure 13). With the effect of a curved Earth instead of a flat one, then the Doppler cell width on the ground is about 290 m along track; however, it is a function of altitude, so it varies. Including also the beam widening effect of the hamming window applied before the azimuth FFT in the processor, then the effective “resolution” of the beams is widened by a factor of roughly 1.3. So the “resolution” (as opposed to sampling) in the along-track direction is more like 380 meters, but this is plus or minus several percent as the altitude varies (see Figure 13).

The width in the across-track direction of the area over which echoes are collected by the antenna (the antenna-limited illuminated area) is approximately equal to 15 km since it can be computed as $2 \cdot h \cdot \tan(\theta/2)$ where h is the altitude and $\theta=1.2^\circ$ the antenna beamwidth across-track. The width in the across-track direction of the area illuminated by the leading edge of the pulse until the time the trailing edge first intersects the surface (the pulse-limited illuminated area around the point of closest approach), in case of almost flat surface response, is equal to $2 \cdot \sqrt{c \cdot h / B}$, approximately 1.6 km for CryoSat, B being the pulse bandwidth.

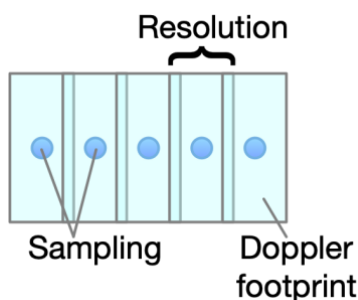


Figure 13: Difference between sampling and Doppler footprint

2.3 Instrument Corrections and Noise

Error components can be characterised according to their time dependence as follows:

- A bias error is a residual fixed offset error, which is stable throughout the mission by definition. Biases are assumed to have a uniform distribution.
- A drift error is a variation due to ageing, or other effects, which appears as a slow change with time, having no periodic character, with the possibility of discrete steps.
- A harmonic error varies periodically, where the period is typically of the order of the orbital or half orbital period but may be much smaller or much longer. The error has a mean of zero.
- A random error varies in an unpredictable manner, relatively quickly in relation to an orbital period, in which there is no correlation between successive realisations. These errors can be assumed as having a Gaussian distribution with zero mean and given standard deviation.

Instrument corrections are derived from characterisation and calibration data. The altimeter's electronic system introduces fixed biases that can be determined during ground-based calibration. For example, perturbations due to differential heating around the orbit cause cyclic and long-term drift, and during the mission are estimated using data from periodic on-board calibrations. The internal path delay correction is a combination of both a fixed part and frequent calibrations. The internal path delay is computed using a specific calibration called CAL1, which is performed for each SIRAL mode about 10 times per week. Physically the path delay is the same for LRM and SAR modes. However LRM data are processed on board where a small shift is added equal to $1/64$ range bin ≈ 7 mm. In order to compensate for this shift, the LRM path delay actually smaller than the SAR one by $1/64$ of the range gate. The path delay values are provided in the L1B products. The L1B product also contains another component of the path delay relative to the waveguides, which is a constant value, measured before launch and common to all modes.

Both antennae require separate corrections for instrument effects on the range (`instr_cor_range_rx_20_ku` and `instr_cor_range_tx_rx_20_ku`) and on the gain (`instr_cor_gain_rx_20_ku` and `instr_cor_gain_tx_rx_20_ku`).

2.3.1 Automatic Gain Control

CryoSat uses Automatic Gain Control (AGC), where information about the previous signal level is used to adjust the gain in anticipation of the next. The aim is to keep the signal level as constant as possible. The actual setting of the on-board receiver attenuator at the observation time is recorded in the L1B products (`agc_ch1_20_ku` and `agc_ch2_20_ku`). The AGC is constant within the radar cycle.

2.3.2 Signal Phase Corrections

Signal phase corrections are split into internal and external types, internal for the electronic system and external for antenna subsystem and waveguide effects. Signal phase is used in SIN mode only.

The corrections are derived from in-flight calibration data. The internal phase correction (`instr_int_ph_cor_20_ku`) is the internal phase correction computed from the latest available CAL-4 packets during the azimuth impulse response amplitude (SIN only).. The external phase correction (`instr_ext_ph_cor_20_ku`) is an external phase correction taken from the IPF database file (SIN mode only) to be added to the internal phase correction term. This is the temperature-averaged component of external inter-channel phase difference derived from phase difference sensitive antenna subsystem, waveguides and instrument waveguide switches. It does not contain internal instrument temperature dependent effects of the calibration coupler and duplexer, which are dealt with by the CAL-4 signal and its subsequent processing and are reported in the internal phase correction parameter.

2.3.3 Phase Slope Correction

Across the whole bandwidth there is a constant change in the phase difference. Some of this was measured before launch; the rest is calibrated at 1Hz. Both measurements are combined to give the phase slope correction (`ph_slope_cor_20_ku`). Since the highest data rate is 20Hz, the closest correction value in time to that of the sample is the one used.

2.3.4 Hamming Weighting Function for SAR Azimuth FFT

A hamming window of length equal to the number of echoes in the burst is generated once at the beginning of the SAR processing, and applied in azimuth direction, to all samples of all echoes of every burst at the very beginning of the beam-forming step. The number of echoes in the burst is always 64 for SAR and SIN.

The windowing process is performed with the following parameters from the processor configuration file:

- `Apply_Azimuth_Hamming`: which defines whether or not apply the window.
- `Azimuth_Hamming_c1` and `Azimuth_Hamming_c2`: which are used to change the shape of the window

$$H(x) = c1 + c2 (\cos((\pi x/N) - (\pi/2)))^2$$

- In the IPF1 processor release VK 1.0 (February 2012) and later (including Baseline D), for both SAR and SIN specialized processors the above parameters are set to:
 - `Apply_Azimuth_Hamming`: on
 - `Azimuth_Hamming_c1`: 0.08
 - `Azimuth_Hamming_c2`: 0.92

When the hamming window is applied, the power is not compensated by any factor. See below the azimuth impulse response of a CAL1 SAR burst, with and without hamming window (zero-padding

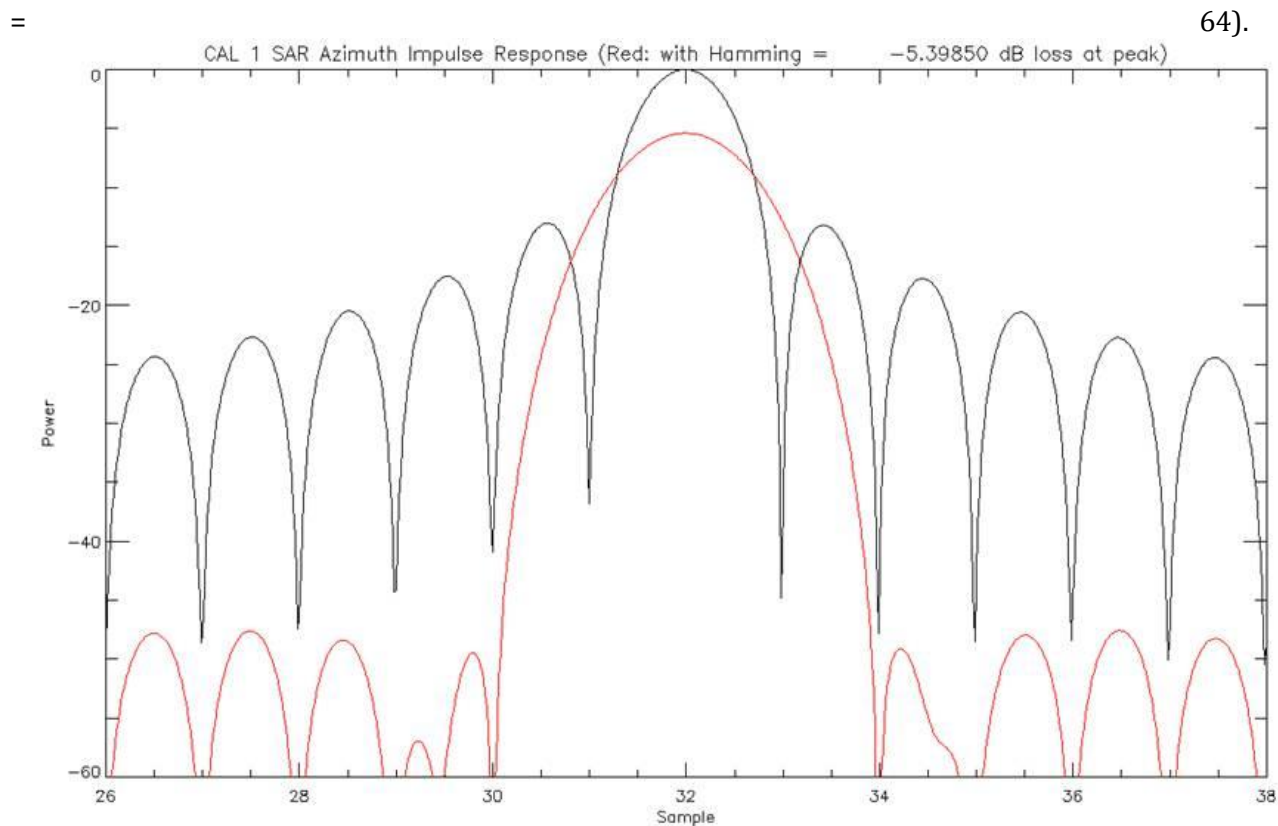


Figure 13: Comparison of Azimuth Impulse Response with and without Hamming window

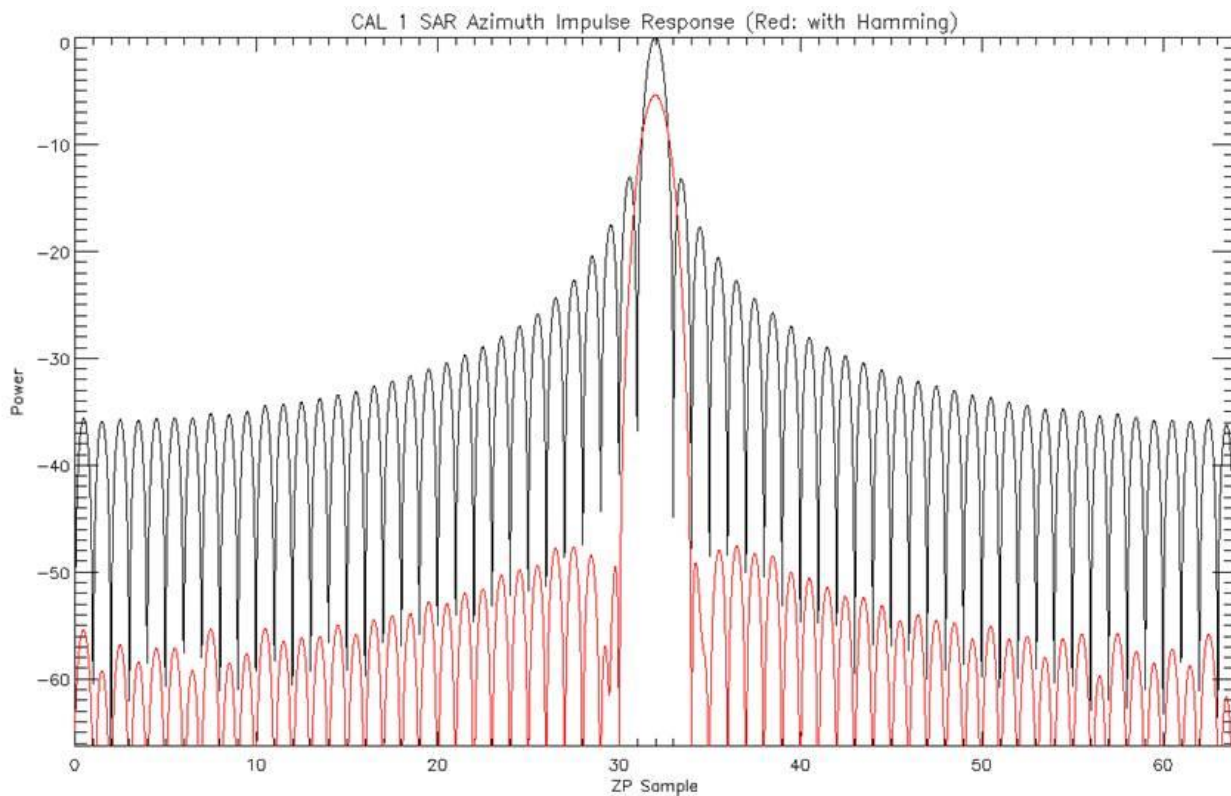


Figure 14: Comparison of Azimuth Impulse Response with and without Hamming window (full range)

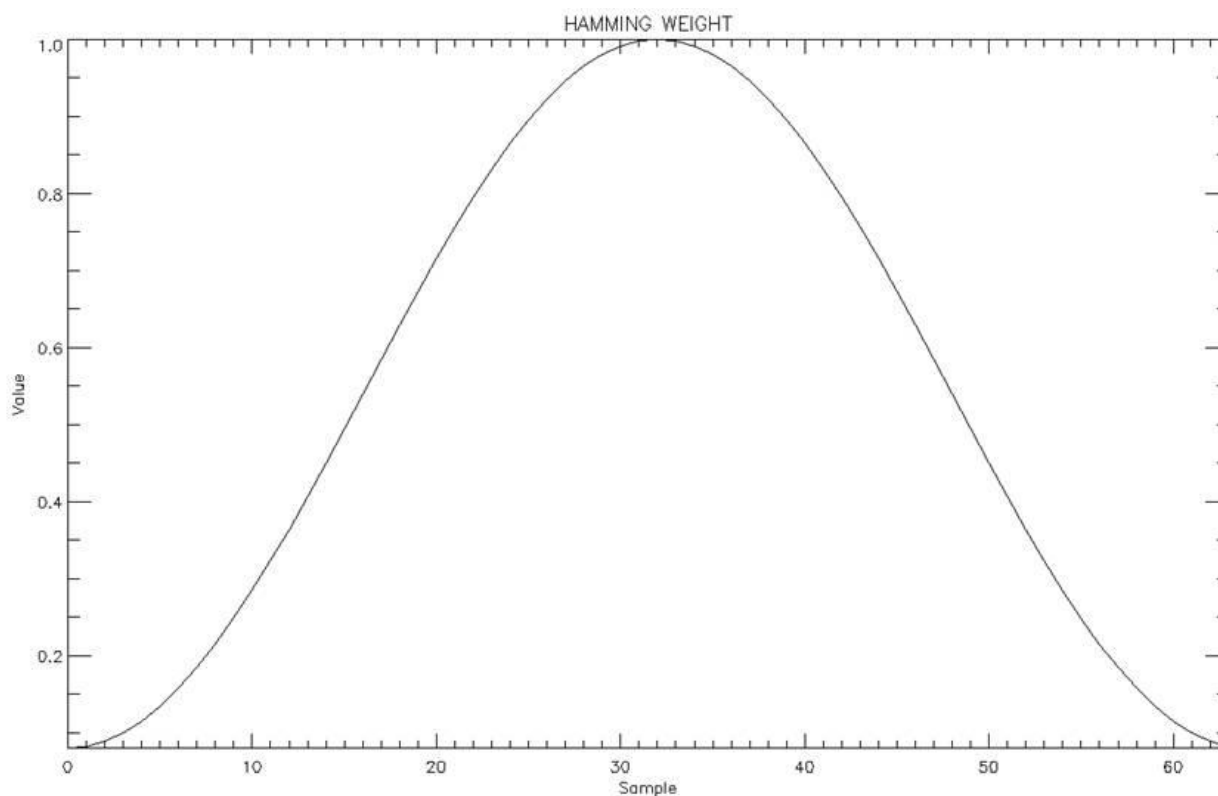


Figure 14: Hamming weighting function

The main beam widening factor is about 1.5 so the azimuth resolution is decreased. The peak power decrease is about 5.4 dB but this should not have any impact on the L2 data. The weighting function aims to reduce the side lobes. This always has the side effect of increasing the main beam width (which means a loss in resolution), and decreasing the main beam power level. There are several weighting functions available. The Hamming weighting function has the characteristic of making the first side lobes very low, reduced by about -42 dB. Hamming is currently used in the processor, in azimuth processing before beam forming (64 beams are created from each burst of 64 waveforms), but this could be changed in the future, if a more suitable function is recommended. It is needed for specular surfaces where the nadir echo is very strong, and beams pointing off nadir contain a strong energy from nadir, which is the clutter in this example. This can be seen in the following four figures for sea ice, showing how the nadir clutter, removed by windowing, can impact the L1B waveform shape and mainly the leading edge.

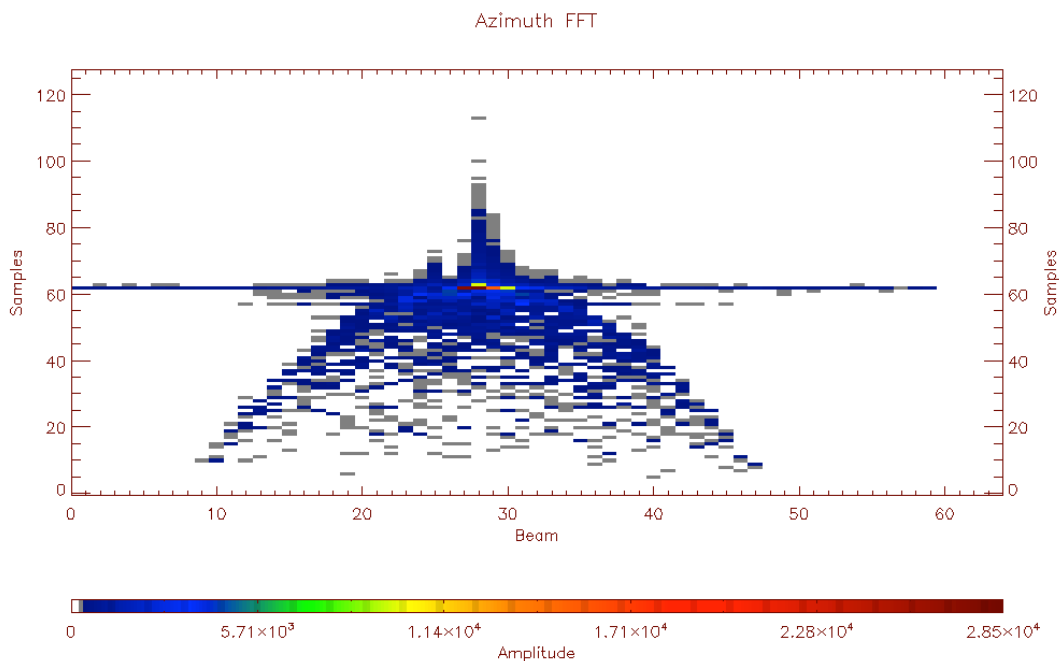


Figure 15: Azimuth FFT of a single burst: the nadir clutter is the 'line' in the middle

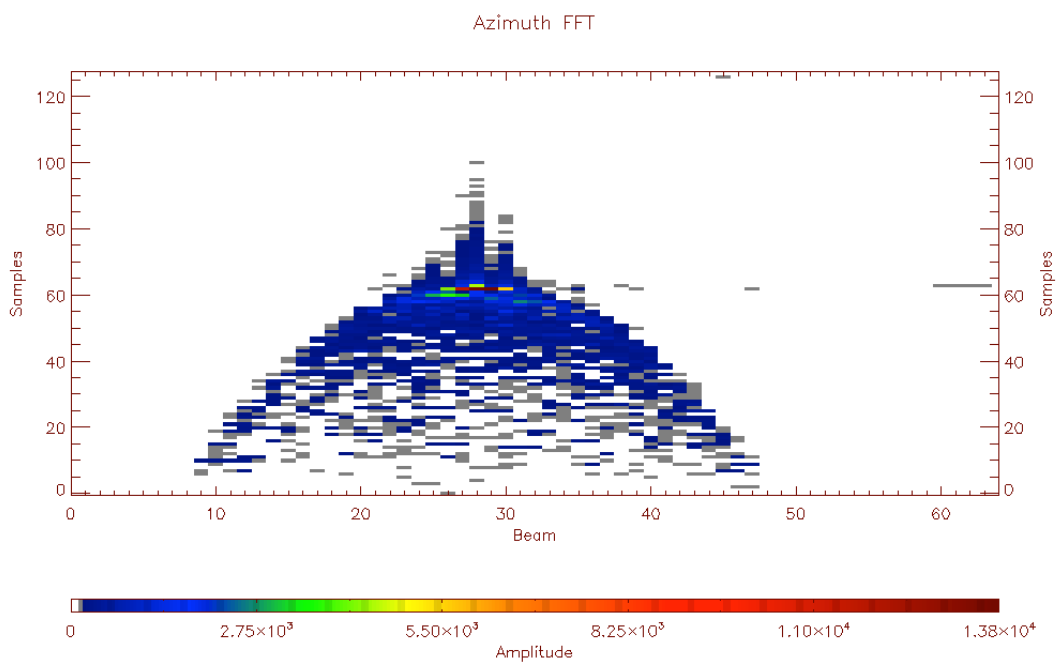


Figure 16: Azimuth FFT of a single burst with hamming: the nadir clutter is reduced

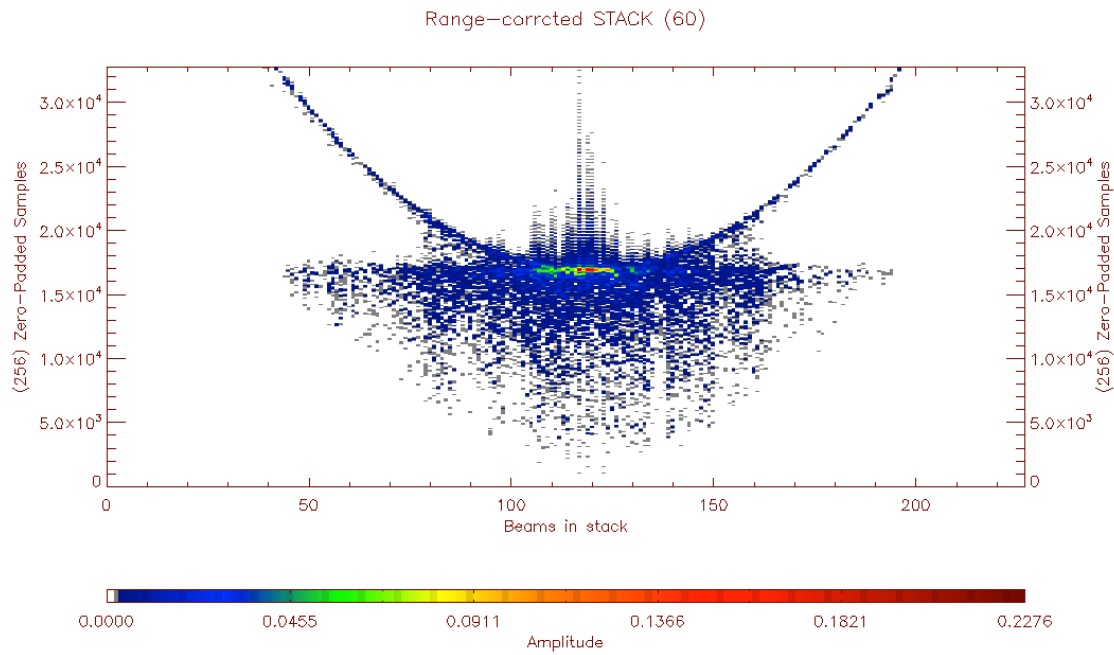


Figure 17: Stack 60 without hamming: here the parabola is the nadir clutter

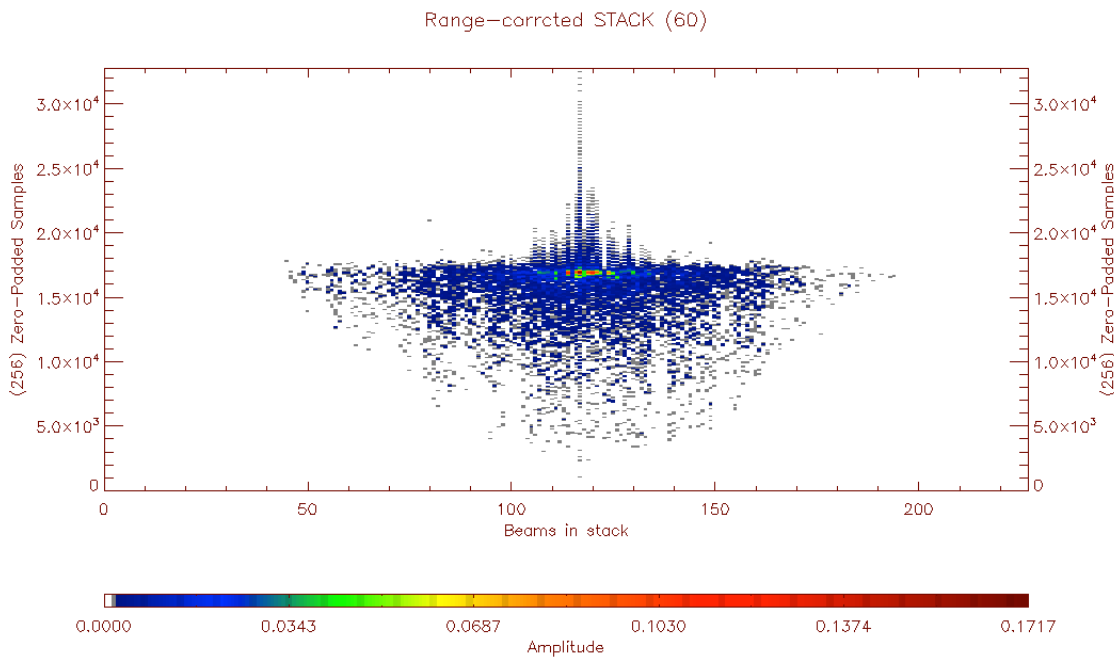


Figure 18: Stack 60 with hamming: the nadir clutter has disappeared

Note that the L1B waveform is obtained by averaging all these beams in the stack.

2.3.5 Noise

Noise on the echo signal is also measured during in-flight calibration (`noise_power_20_ku`). At L1B, an estimate of the noise is given as the noise power measurement, but it is not subtracted from the waveforms. At L2, noise is re-estimated as part of the retracking calculations. In SIN mode, this estimate is subtracted from the bin power before the retracking is performed.

2.3.6 Echo Saturation

Echo saturation occurs when the power in the pulse varies more than the dynamic range of the receiver, causing distortions in the echo waveform. This mostly occurs in high-amplitude echoes from flat bright surfaces such as leads in sea ice or melt ponds on ice sheets. This condition is flagged in the measurement confidence data (MCD) of L1B and L2 products (`flag_mcd_20_ku`) using the flag “echo_saturated”.

2.3.7 Doppler Correction

When there is a component of the satellite orbital velocity vector directed along the line of sight from the satellite to the echoing point on the surface, the radar echo undergoes a corresponding Doppler shift. This is compensated by a Doppler range correction (`dop_cor_20_ku` in L1b). All range corrections are defined such that they are added to the range measurement to give the true range.

2.4 Retracking and Parameters Derived from Echo Shape

2.4.1 Range Window and Window Delay

The distance between the satellite and the Earth surface varies around its orbit by several kilometres. However, in the vertical dimension the altimeter can only receive echoes within a ‘range window’ specified by the width of the frequency spectrum.

Prior to the Baseline-C Ice processor the L1B range window values were set to 128 for LRM, 128 for SAR and 512 for SIN. However these window values truncated part of the L1B waveform. At Baseline-C, the L1B range window values were increased to fully capture the whole waveform. Therefore from Baseline-C onwards the L1B range windows were updated as follows: 128 for LRM; 256 for SAR; 1024 for SIN.

In order to receive echoes all around the orbit, the time of the reception period must be continuously adjusted to try to keep a specific point on the leading edge of the echo waveform at a reference position within the window. The CryoSat reference position is configurable, but it is for now centrally located, at bin 64 of the range window in LRM mode, bin 128 in SAR mode, and at bin 512 in SIN mode (bins are counted from bin 0). The window delay (`window_del_20_ku` in L1B) refers to the 2-way time between the pulse emission and the reference point at the centre of the range window.

2.4.2 Reception Period

Information about the reception period time is represented in two ways. Either an initial height is given (`h0_applied_20_ku` in L1B), followed by the rate of change in this height per tracking cycle (`cor2_applied_20_ku` in L1B), or a coarse height (`h0_lai_word_20_ku` in L1b) and fine height adjustment (`h0_fai_word_20_ku` in L1B) are given, which must be added together. The tracking cycle is a fundamental interval common to all modes, of 47.2 ms.

2.4.3 Range Window Sampling

In LRM, the range window explored is about 60 m, covered by 128 data samples. In SAR mode it is about 60 m, covered by 256 data samples. In SIN mode, due to the slope variation in ice sheet margins, the range window is increased to about 240 m, and is covered by 1024 samples. During processing the exact, calibrated, length of the data bins is retrieved from the instrument characterisation data file, the filename of which is found in the Dataset Description (DSD) in the header file, or global attributes section of the data file.

There are two types of waveforms provided in the LRM, SAR and SIN L1B products.

1. Waveforms derived from classical LRM or those generated from SAR/ SIN azimuth processing that are provided in the L1B products (`pwr_waveform_20_ku`)
2. Pulse-width limited data extracted from all modes averaged over 1 second and provided in the L1B products (`pwr_waveform_avg_01_ku`)

It is a fact that radar altimeter power echo waveforms are aliased (see [RD 28])

During the CryoSat commissioning phase, it became clear that SAR processed data over specular surfaces was aliased. This was particularly evident when the rate of change of satellite altitude was large, and as a result SAR (and SIN) L1B data was highly degraded over specular surfaces.

In general, the aliasing effect appears minor over diffuse surfaces such as ocean but is nevertheless present. In order to avoid aliasing, raw complex SAR and SIN echoes are now oversampled (since 01/02/2012, Baseline-B) in the FBR to L1B processor and as a result data users need to take this into account when using waveforms and determining range. Although the sampling has changed, the resolution has not changed since it is fixed by the instrument impulse response.

LRM sampling remains the same as in earlier versions of the CryoSat processors as sampling is fixed on-board and oversampling of the on-board complex data is not possible. However, LRM data is affected by aliasing as in other altimeter missions.

What follows is a description of how to compute the range to a given range bin for all cases.

For ALL LRM 20 Hz and ALL 1Hz data:

Given the waveform array, $\Phi(n)$ (`pwr_waveform_avg_01_ku` or `pwr_waveform_20_ku`) where n is the waveform sample number with a value $\forall n \in [0, N_s - 1]$ (any value between 0 and $N_s - 1$) and N_s is the mode dependent number of samples in any waveform:

$$N_s = \begin{cases} 128, LRM \\ 256, SAR \\ 1024, SIN \end{cases}$$

The range $R(n)$ to waveform sample n is given by $R(n) = \frac{T_w c}{2} - \frac{N_s c}{4B} + \frac{nc}{2B} = \frac{c}{2B} (T_w B - \frac{N_s}{2} + n)$ [m], where T_w is the window delay converted to seconds (`window_del_avg_01_ku` or `window_del_20_ku`) referenced to the central range bin $n = \frac{N_s}{2} = 64$, the first range bin being $n = 0$, c is the speed of light in vacuum, $c = 299792485.0$ m/s, B is the measured chirp bandwidth, $B = 320,000,000$ Hz.

Hence, the range to the first waveform sample, $n = 0$ is $R(0) = \frac{T_w c}{2} - \frac{N_s c}{4B}$ meters.

Each waveform sample covers a range of $\Delta R = \frac{c}{2B} = 0.4684$ m $\Delta r = \frac{c}{2B} = 46.84$ cm or a delay of $\Delta t = \frac{1}{B} = 3.125$ ns.

For SAR and SIN 20 Hz oversampled echoes in products generated with Ice Baseline-C and later:

Given the oversampled power echo waveform array, $\Phi(n)$ (`pwr_waveform_20_ku`) where n is the waveform sample number with a value $\forall n \in [0, N_s - 1]$ (any value between 0 and $N_s - 1$) and N_s is the mode dependent number of samples in any waveform:

$$N_s = \begin{cases} 256, SAR \\ 1024, SIN \end{cases}$$

The range $R(n)$ to waveform sample n is given by $R(n) = \frac{T_w c}{2} - \frac{N_s c}{8B} + \frac{nc}{4B} = \frac{c}{8B} (4T_w B - N_s + 2n)$ [m]

where T_w is the window delay converted to seconds (`window_del_20_ku`) referenced to the central range bin $n = \frac{N_s}{2}$, the first range bin being $n = 0$, c is the speed of light in vacuum, $c = 299792485.0$ m/s, B is the measured chirp bandwidth, $B = 320,000,000$ Hz.

Hence, for example, the range to the first waveform sample, $n = 0$ is $R(0) = \frac{T_w c}{2} - \frac{N_s c}{8B}$ meters.

Each waveform sample covers a 1-way range of $\Delta R_{os} = \frac{c}{4B} = 0.2342$ m $\Delta r = \frac{c}{2B} = 46.84$ cm or a delay of $\Delta t = \frac{1}{2B} = 1.5625$ ns (two-way time).

2.4.4 Echo Positioning and Scaling

In the data products the position of the echo within the range window varies with SIRAL mode. The instrument dynamically sets the range window and in LRM the window position is not changed by the data processing. In SAR and SIN modes echoes are averaged during data processing on the ground and the position of the window is then selected to best accommodate the resultant waveform.

In order to retain as much information as possible, the individual samples of each echo waveform are scaled to fit within the range 0 to 65535. They can be converted to power in watts using with the L1B parameters `echo_scale_pwr_20_ku` and `echo_scale_factor_20_ku` (or `echo_scale_pwr_avg_01_ku` and `echo_scale_factor_avg_01_ku`) as follows

$$\text{scaled_waveform} = \text{waveform} * \text{echo_scale_pwr_20_ku} * 2^{\text{echo_scale_factor_20_ku}}$$

2.4.5 Retracking

At L2, a procedure commonly referred to as retracking is performed. A specific point on the echo's leading edge, known as the retracking point, is used to mark the point of measurement of range to the surface. The retracking point is defined relative to the shape of the whole echo and found using a model-fitting method. The offset of the retracking point from the reference point (corresponding to the 2-way window delay), which for CryoSat is in the centre of the range window, is then calculated. This is the retracking correction.

The algorithms used for retracking vary with mode. Table 4 provides the current retrackers used in the Ice Baseline-D processors.. For LRM (any surface type), the amplitude and epoch returned by the Offset Centre Of Gravity (OCOG) retracking performed upon the waveform, are used as the initial guesses for the fits performed by the Ocean CFI and land-ice retrackers. The primary results are returned in the height variables (`height_1_20_ku`, `height_2_20_ku`, and `height_3_20_ku`). These heights are fully corrected for all appropriate instrumental and geophysical corrections, and any known residual biases.

Table 4: Retrackers used in Baseline-D Ice processor

Retracker ID	Mode LRM	Mode SAR	Mode SARin
1	Ocean CFI model fit	UCL sea-ice: Diffuse echo - CPOM threshold of first peak Specular echo - Giles model fit	UCL margins: Wingham/Wallis model fit
2	UCL land-ice	not used	not used
3	OCOG	not used	not used

The CLS Ocean CFI retracker and UCL land-ice retracker are model-fits to the LRM waveform. The ocean retracker fits a Hayne model waveform that is not adapted for CryoSat and the UCL retracker fits a Brown model adapted for CryoSat [RD 19]. Further details of retrackerers are given in [RD 16], and background information in [RD 3][RD 17]. OCOG is well described in the literature ([RD 20]).

For SAR mode, the retracker is a model fit for specular lead waveforms, and a threshold retracking to the first peak of a smoothed waveform for diffuse echoes from sea-ice. In SIN mode, the Wingham/Wallis retracker fits a theoretical model to the portion of the power waveform that exhibits the maximum coherence. The phase difference is estimated at the retracking point to give the across-track angle of the echoing point. The SAR mode retracking is also performed on the SIN waveforms, with the results appearing in variables `height_sea_ice_floe_20_ku` (diffuse) and `height_sea_ice_lead_20_ku` (specular).

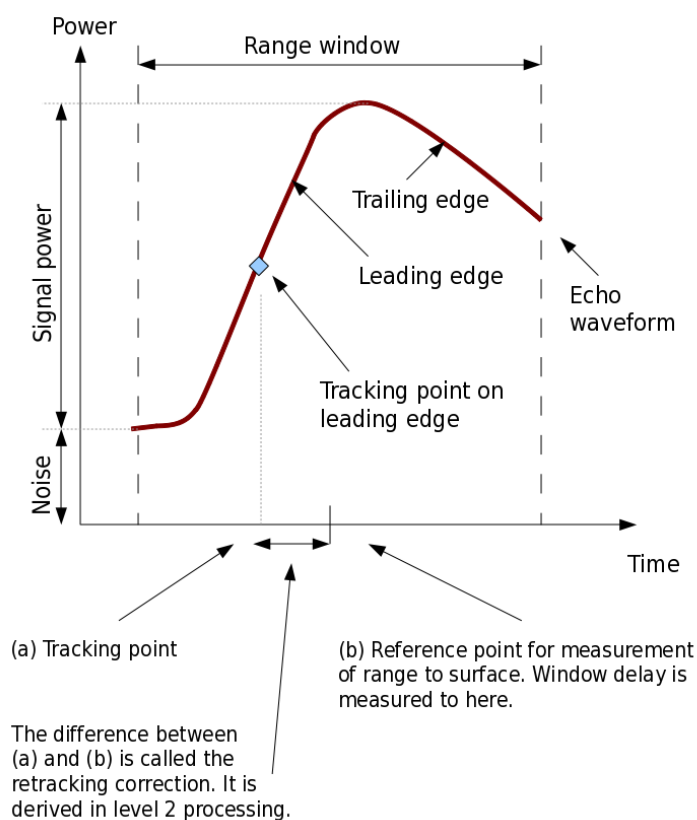


Figure 19: Idealised pulse-limited waveform in window

In the L2I products, retracker corrections to range which have been applied during retracking are provided for each of the (up to) three retrackerers (`retracker_1_cor_20_ku`, `retracker_2_cor_20_ku`, and `retracker_3_cor_20_ku`).

The L2I products also contain the range with only retracking and instrumental corrections applied (`range_1_20_ku`, `range_2_20_ku`, and `range_3_20_ku`). This allows the user to apply their own geophysical corrections directly, rather than removing and reapplying.

2.4.6 Backscattering

The radar backscattering coefficient (σ_0) provides information about the observed surface. It is a function of the radar frequency, polarisation and incidence angle and the target surface roughness, geometric shape and dielectric properties. A discussion of all these factors is given online

at

http://earth.esa.int/applications/data_util/SARDOCS/spaceborne/Radar_Courses/Radar_Course_I/parameters_affecting.htm

At L2, the backscatter coefficient is fully corrected, including instrument gain corrections and an empirically derived bias correction. A measurement is made for each retracker ($\text{sig}\theta_{1_20_ku}$, $\text{sig}\theta_{2_20_ku}$, and $\text{sig}\theta_{3_20_ku}$). See [RD 22] for background information.

2.4.7 Peakiness

Peakiness is a measure of how sharply peaked an echo is (peakiness_{20_ku}). It is essentially the ratio of the highest bin value to the mean value of all bins (or mean of all bins above the noise floor in SAR mode). The higher the ratio, the more peaked the echo. High peakiness indicates a very specular reflection, such as that from leads in sea ice. Further information is given in [RD 21].

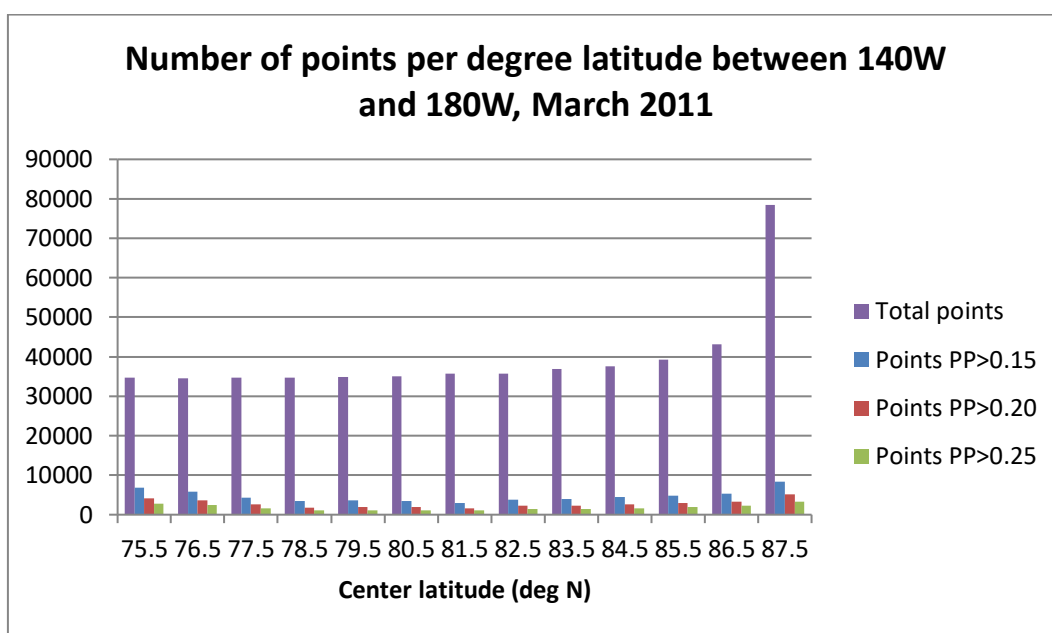


Figure 20: Peakiness by latitude

The figure above shows the total number of points available per degree latitude, between 140W and 180W for March 2011 along with the number of points with ‘Pulse Peakiness’ (PP) above certain thresholds. Higher PP indicates more ‘specular’ waveforms i.e. waveforms more likely to originate from leads. The total number of CryoSat measurements between 75N and 88N (between 140W and 180W) is 515000.

The figure below shows the number of points with PP greater than certain thresholds as a proportion of the total number of points recorded, per degree latitude, for March 2011. The number of points varies with latitude according to the proportion of sea ice cover, as well as, presumably, climatological conditions.

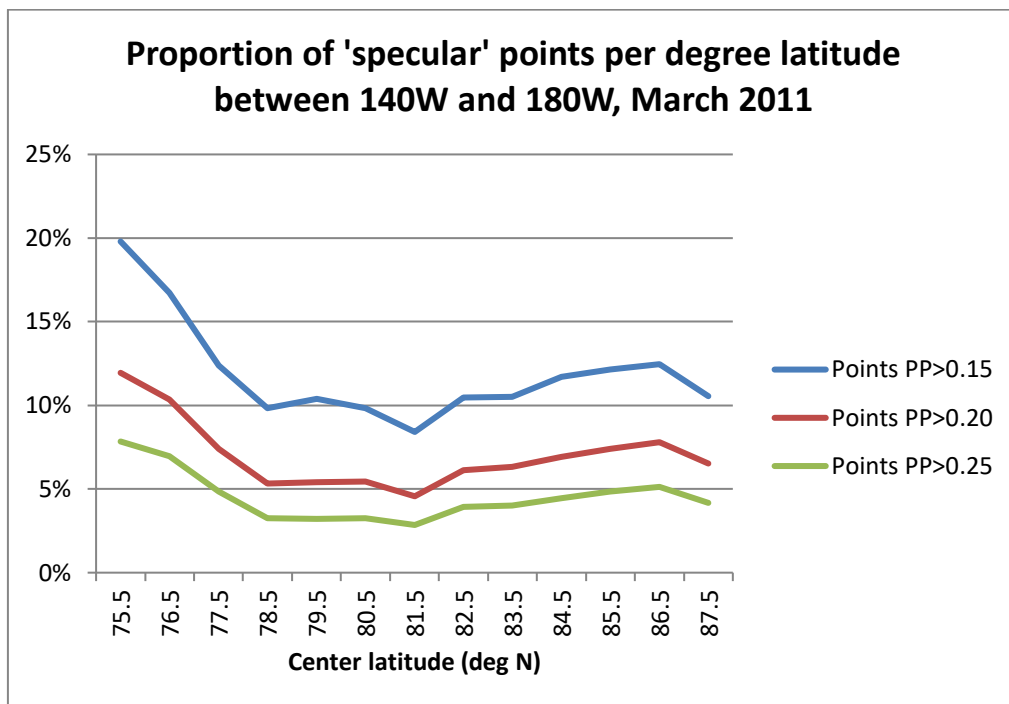


Figure 21: Proportion of specular points by latitude

2.4.8 Interferometric Mode Specific Parameters

The purpose of the SIN mode is to allow the across-track angle offset of the echoing point to be determined directly (using interferometric phase information). In the L2 SIN products, the 20Hz latitude (`lat_poca_20_ku`) and longitude (`lon_poca_20_ku`) values provide the estimated position of the point of closest approach (as computed from the phase difference) and not the nadir. The nadir location is only present in the L2 products at 1Hz (`lat_01` and `lon_01`). Each 20Hz sample produces only one location on the ground.

It is important to note that phase-wrapping can occur when the across track offset is great enough and this can have the effect of the echo appearing to come from the other side of the ground track. Normally, this is flagged (`flag_sarin_ambiguity_warning_20_ku`) by use of an ambiguity Digital Elevation Model (DEM; `dem_height_20_ku`) that shows where this effect is likely to have occurred, however these DEMs are only available for Greenland and Antarctica. This test is not switched off when the satellite is over the ocean as the instrument may still be tracking the land. This may mean that ocean data is flagged as 'ambiguous' in some cases. Users should be aware of this, and ignore the ambiguity flag where appropriate if they are using ocean data.

If the user observes a sequence of records with increasing across-track offset and then an abrupt switch to the other side of the track, it is possible that phase-wrapping has occurred.

2.4.9 Significant Wave Height

Significant wave height (SWH) `swh_ocean_20_ku` is the average wave height, trough to crest, of the one-third largest waves in a particular geographic location. SWH can be derived from inspection of the echo waveform. The reflection from the wave crest is returned earlier than that from the trough, 'stretching' the leading edge of the waveform. The stretching increases with increasing wave height. This computation can produce negative values for SWH if the leading edge is steeper than the model expects. These values are preserved in the product, rather than being set to zero, so that the correct distribution of the values is maintained. They are physically meaningless, but some users choose to apply a bias correction which can render them positive.

2.4.10 Wind Speed

The CryoSat L2 data includes wind speed calculated from the radar backscattering coefficient using the Abdalla 2007 model (see [RD 7]).

2.4.11 Geophysical Corrections by Surface

The geophysical corrections included and applied in the L2 products depend on the product and surface type. **Error! Reference source not found.** below lists the main L2 product characteristics and the necessary geophysical corrections over each surface type in order to retrieve corrected elevations. For Offline L2 products from the CryoSat Ice Processor, the relevant corrections are applied to the range. Sections 2.5 and 2.6 describe in detail the geophysical corrections (see also [RD 8] and [RD 26]).

2.4.12 Surface Type

The L1B and L2 products contain a flag word to classify the surface type at nadir. This classification is derived using a four state surface identification grid, computed by combining data from different sources: GMT, GlobCover, Modis Mosaic of Antarctica, and Water body outlines from LEGOS. The grid provides four states of the flag: 0 = open oceans or semi-enclosed seas; 1 = enclosed seas or lakes; 2 = continental ice; 3 = land.

Note that the surface type flag at L1B is provided at 1 Hz resolution (`surf_type_01`), whilst the flag provided at L2 is provided at 20 Hz resolution (`surf_type_20_ku`). The surface type flag is used to determine the set of appropriate geophysical corrections to apply (Table 5).

Table 5: Geophysical Corrections applied to Level 2 products over each surface type

Products Mode	Surface type	Ocean surface corrections	Tidal corrections	Atmospheric propagation corrections
Offline LRM	Ocean	DAC Sea State Bias	Ocean Tide Long Period Equilibrium Tide Ocean Loading Tide Solid Earth Tide Geocentric Polar Tide	Dry Tropospheric Wet Tropospheric Ionospheric
Offline LRM	Interior Land Ice	Not applied	Ocean Loading Tide Solid Earth Tide Geocentric Polar Tide	
Offline SIN	Margin Land Ice	Not applied		
Offline SAR	Sea Ice	Inverse Barometric correction	Ocean Tide Long Period Equilibrium Tide Ocean Loading Tide Solid Earth Tide Geocentric Polar Tide	

2.5 Range Corrections for Atmospheric Effects

An altimeter pulse slows down slightly as it passes through the Earth's troposphere due to the refractive properties of the atmosphere. When the time delay is converted to range, using the speed of light in a vacuum, this small additional delay must be accounted for via a number of propagation

corrections. The speed of light used in the CryoSat processor is 299792458.0 metres per second. Some corrections are also necessary to account for the ocean's response to atmospheric forcing and are removed from the sea surface height.

2.5.1 Dry and Wet Tropospheric Corrections

The dry tropospheric correction (`mod_dry_tropo_cor_01`) is the correction for refraction due to the dry gas component of the atmosphere, and compensates for the effect of non-polar gases such as oxygen and nitrogen, which delay the radar return signal. It has a typical range from 1.7 to 2.5 m.

For CryoSat, this correction is not received via a direct ADF input. Instead this correction is computed by the CryoSat processors using dynamic mean surface pressure Meteo grids sourced from Meteo - France via the Systeme au Sol d'ALTimetrie et d'Orbitographie (SSALTO) based on the European Centre for Medium-Range Weather Forecasts (ECMWF) model, as well as static S1 and S2 tide grids of monthly means of global amplitude and phase. These static tide grids for amplitude and phase have latitude coverage from -90 to +90 degrees and a step in latitude/longitude of 1.125 degrees (see [RD 7]).

For the Dry Tropospheric Correction over water (open water, semi-enclosed seas or enclosed seas and lakes), the surface pressure is equal to the mean pressure minus the climatology (computed with the pressure grids). Over land, the surface pressure is equal to the mean pressure so the Dry Tropospheric Correction over land is computed from the mean pressure alone.

The wet tropospheric correction (`mod_wet_tropo_cor_01`) is the correction for the path delay in the radar return signal due to the effect of polar gases in the atmosphere, mainly water vapour. It has a typical range from 0 to 50 cm.

For CryoSat, this correction is provided by Meteo grids, sourced from Meteo-France via SSALTO and is based on the ECMWF model. The Wet Tropospheric Correction is received as a direct ADF input from ECMWF analysed grids and is then formatted to the CryoSat Payload Data Segment (PDS) file standard before being used by the CryoSat processor ([RD 15]).

2.5.2 Ionospheric Correction

The Ionospheric Correction takes into account the path delay in the radar return signal due to the free electron content of the ionosphere. There are two sources currently used to derive this correction for CryoSat; the Global Ionospheric Map (GIM) and the Bent model.

Computation of the GIM correction requires Global Positioning System (GPS) ionospheric data computed every second along the satellite tracks. This is sourced from Centre National d'Etudes Spatiales (CNES) via SSALTO as a dynamic daily ADF.

The Bent Model correction is derived using two static files, the Bent Ionospheric Coefficients file and the Bent Modified Dip Map, provided by Collect Localisation Satellites (CLS). In addition, the Bent Model Ionospheric Correction also requires the Solar Activity Index, provided as monthly files by CNES (defined in [RD 4]). It should be noted that the Bent Model is not available for latitudes greater than ± 82 degrees and is only provided as a backup in the event the GIM is not available.

L1B Offline products currently contain the Ionospheric Correction values derived from both the GIM (`iono_cor_gim_01`) and Bent Models (`iono_cor_01`). At L2, only the Ionospheric Correction value which is applied to the range is provided. The use of the Ionospheric GPS Grid is now mandatory for all Offline production, and is used to compute the GIM Ionospheric correction in all cases.

2.5.3 Inverse Barometric Correction

The inverse barometric correction (`inv_bar_cor_01`) compensates for variations in sea surface height due to atmospheric pressure variations (atmospheric loading). It has a typical range from -15 to +15 cm and is calculated using dynamic surface pressure files sourced from Meteo-France via SSALTO, based on ECMWF outputs, as well as static S1 and S2 tide grids of monthly means of global amplitude and phase (see [RD 7]/[RD 26]).

This correction is only used in SAR mode and where the surface type is “open ocean”. It should not be used over land, enclosed seas or lakes.

2.5.4 Dynamic Atmospheric Correction

The Dynamic Atmospheric Correction (DAC; `hf_fluct_total_cor_01`) is needed to correct for the depression of the ocean surface caused by the local barometric pressure and winds. It has a typical range from -15 to +15cm. The correction is a combination of the high frequency, high resolution 2D Gravity Waves Model (MOG2D), an ocean model forced by ECMWF atmospheric parameters after removing S1 and S2 atmospheric tides, and the low frequency Inverse Barometric (IB) Correction. The DAC correction is provided by Meteo grids taken from the barotropic MOG2D model [RD 23] and is sourced from CNES via SSALTO.

For the CryoSat Ice processor, this correction is used over ocean only where there is no sea-ice cover, i.e. for LRM and in a very few cases for SIN mode when the surface type is “Open Ocean”. This is because the DAC model does not take into account the dampening effect of sea ice cover on the wind forcing. It should not be used over land, enclosed seas or lakes.

2.5.5 Sea State Bias

Sea state bias (SSB) or Electromagnetic (EM) Bias is the correction for bias in the measurements introduced by varying reflectivity of the crests and troughs of the sea surface. Wave troughs are better reflectors of energy than wave crests, due to their different distributions of specular-reflecting facets, thus the centroid of the mean reflecting surface is shifted away from the mean sea surface towards the troughs of the waves. The SSB correction given in the L2 data (`sea_state_bias_20_ku`) is an empirical correction proportional to the significant wave height which compensates for the asymmetric shape of ocean waves and is derived from a model provided by CLS to ESA (see [RD 12]).

2.5.6 Derivation of Corrections

Most of the above corrections are provided on a Meteo grid, a group of 6 dynamic files containing grids of surface pressure, ocean mean-sea-level pressure, wet and dry tropospheric corrections and U (east-west) and V (south-north) wind components. In addition a static file for the grid definition is required. This is the Gaussian Altimetric Correction Grid. Each Meteo grid covers a 6-hour period. Two Meteo grids are required for the computation of a correction: one before and one after the product validity time. These grids are interpolated in time and space in order to derive a correction value for each measurement. These files are further defined in [RD 7].

2.5.7 Application of Corrections to Range

The above corrections are added to the range measurement to give the true range. Further background information is given in [RD 8].

2.6 Range Corrections for Tidal Effects

Tidal corrections are required to adjust the range to appear as if it originates from the mean ice or land surface, or tide-free sea surface. In the L1B products, the “ocean tide” field does not include the

loading tide or the long period tide. For the L2 product, the users do not need to apply any tides as they are applied during the computation of height. However, if they are working with the L1B product and deriving their own surface height then they should apply the set of tides and meteorological corrections in the L1B that is suitable for their specific usage.

2.6.1 Ocean Tide

The Ocean Tide Correction (`ocean_tide_01`) removes the effects of local tides, i.e. those caused by the Moon, and typically ranges from -50 to +50 cm. In Level 2 Offline products (from the CryoSat Ice Processor) the Ocean tide correction is computed using a static file, derived from the Finite Element Solution 2004 (FES2004) tide model, which has latitude coverage from -90 to +90 degrees and a step in latitude/longitude of 0.125 degrees. In these products the Ocean Tide does not include the Ocean Loading Tide or the Long-Period Equilibrium Tide, and these are provided separately (see below).

The FES2004 Ocean Tide Model [RD 24], is a global hydrodynamic tide model initiated by the works of Christian Le Provost in the early nineties. It is based on the resolution of the tidal barometric equations on a global finite element grid (~1 million nodes), which leads to solutions independent of the in situ and remote-sensing data (no open boundary condition and no assimilation data). A new original high-resolution bathymetry was used and ice in Polar Regions was taken into account. The accuracy of these 'free' solutions was improved by assimilating tide gauge and altimetry data (TOPEX/Poseidon (T/P) and ERS-2) through a revised representer assimilation method (<http://www.aviso.oceanobs.com/index.php?id=1279>).

2.6.2 Long-Period Equilibrium Ocean Tide

The Long-Period Equilibrium Tide correction (`ocean_tide_eq_01`) removes the effects of low frequency local tides caused by the gravitational attraction effects. The long-period tides, with a period greater than 2 weeks, have amplitudes of less than 1 cm and on theoretical grounds have generally been thought to approximate to static equilibrium in the ocean [RD 25]. In the Level 2 Offline products (from the CryoSat Ice Processor) the correction is computed using a static file, derived from the FES2004 tide model [RD 24], which has latitude coverage from -90 to +90 degrees and a step in latitude/longitude of 0.125 degrees.

2.6.3 Ocean Loading Tide

The Ocean Loading Tide correction (`load_tide_01`) removes the deformation of the Earth's crust due to the weight of the overlying ocean tides. Typically this correction ranges from -2 to +2 cm. In the Level 2 Offline products (from the CryoSat Ice Processor) the correction is computed using a static file, derived from the FES2004 tide model [RD 24], which has latitude coverage from -90 to +90 degrees and a step in latitude/longitude of 0.25 degrees. This is further described in [RD 7]. Note that the effect of ocean tide loading on the Earth's crust propagates inland (at least for near coastal areas), and therefore the loading tide correction needs to be applied over land surfaces as well. It is not known how well the model manages this effect.

2.6.4 Solid Earth Tide

The Solid Earth Tide correction (`solid_earth_tide_01`) removes the deformation of the Earth due to tidal forces from the Sun and Moon acting on the Earth's body. Typically, this correction ranges from -30 to +30 cm. The correction is computed using a static file, derived from the Cartwright tide model [RD 9].

2.6.5 Geocentric Polar Tide

The Geocentric Polar Tide correction (`pole_tide_01`) accounts for the ocean's response to the long-period distortion of the Earth's crust caused by variations in the centrifugal force during

perturbations in the Earth’s rotational axis. Typically, this correction ranges from -2 to +2 cm. The correction is derived using dynamic Instantaneous Polar Location files, which comprise the historical pole positions and are provided as daily dynamic files sourced from CNES via SSALTO. It is further described in [RD 7]/[RD 26].

2.6.6 Application of Corrections to Range

The above corrections are added to the range measurement to give the true range. For further information see [RD 8].

2.6.7 Additional Corrections not applied to Range

Some further corrections (or values needed to compute corrections), not applied in the IPF processing, can be applied by users if desired. To facilitate this the L2 products contain some additional geophysical parameters coincident with Cryosat measurements. These are: snow depth and snow density. See Table 6.

2.7 Models Used

2.7.1 Static Auxiliary Data Files

This table below provides details of the static auxiliary data files used in processing of CryoSat data products. These files are referred to as static because they have fixed “start” and “stop” times which cover the entire mission duration. During processing space and time interpolation is performed along the CryoSat track location. The “grid” type files have data distributed on a geographical grid, whereas the “data” type files are non-geographical.

Table 6: Static auxiliary data files

File Type	Description	Type	Parameters (grid only)
			All longitude coverage is [0,360] degrees
AUX_CARTWR	Cartwright and Edden tables	Data	N/A
AUX_DEMMSL	MSSL high-resolution DEMs of Greenland and Antarctica	Grid	Cartesian grids covering Antarctica, grid step = 1km, and Greenland, grid step = 800m
AUX_DIPMAP	Bent Modified Dip Map file	Grid	Latitude coverage: [-88,88] degrees Step in latitude: 2 degrees Step in longitude: 2 degrees
AUX_GEOID_	EGM96 Geoid values	Grid	Latitude coverage [-88,88] degrees Step in latitude: 0.25 degrees Step in longitude: 0.25 degrees
AUX_LS_MAP	Four states surface identification grid from combination of data: GMT, GlobCover, Modis Mosaic of	Grid	Latitude coverage: [-90,90] Step in Latitude: 1/30 degrees Step in longitude: 1/30 degrees

	Antarctica, and Water body outlines from LEGOS		
AUX_MICOEF	Bent Ionospheric Coefficients File	Data	N/A
AUX_MSSURF	Mean Sea Surface from UCL13 model	Grid	Latitude coverage: [-80,88] degrees Step in latitude: 0.0625 degrees Step in longitude: 0.0625 degrees
AUX_OCTIDE	FES2004 Ocean Tide Model	grid	Latitude coverage: [-90,90] degrees Step in latitude: 0.125 degrees Step in longitude: 0.125 degrees
AUX_ODLE_	MACCESS Ocean Depth/Land Elevation	Grid	Latitude coverage: [-90,90] Step in Latitude: 1/30 degrees Step in longitude: 1/30 degrees
AUX_PRSS00 AUX_PRSS06 AUX_PRSS12 AUX_PRSS18	Climatology pressure grids, four per day, for 0h, 6h 12h and 18h. Each grid point contains 12 values of climatological pressure, one for each month of the year	Grid	Latitude coverage: [-90,90] degrees Step in latitude: 0.5 degrees Step in latitude: 0.5 degrees
AUX_S1AMPL AUX_S2AMPL	The S1 and S2 tide grids of monthly means of global amplitude. Each grid point contains 12 values of amplitude, one for each month of the year	Grid	Latitude coverage: [-90,90] degrees Step in latitude: 1.125 degrees Step in latitude: 1.125 degrees
AUX_S1PHAS AUX_S2PHAS	The S1 and S2 tide grids of monthly means of global phase. Each grid point contains 12 values of phase, one for each month of the year.	Grid	Latitude coverage: [-90,90] degrees Step in latitude: 1.125 degrees Step in latitude: 1.125 degrees
AUX_SDC_nn	UCL04 Snow Depth Climatology model (nn= month number)	Grid	Latitude coverage: [0,90] degrees Step in latitude: 0.0625 degrees Step in longitude: 0.0625 degrees
AUX_SICCnn	UCL04 Sea Ice Concentration Climatology (nn= month number)	Grid	Latitude Coverage: [-90,90] degrees Step in latitude: 0.0625 degrees Step in longitude: 0.0625 degrees

AUX_SLPMSL	MSSL High resolution Slope models of Greenland and Antarctica	grid	Cartesian grids covering Antarctica, grid step = 1km, and Greenland, grid step = 800m
AUX_TDLOAD	FES2004 Tidal Loading Model	Grid	Latitude coverage: [-90,90] degrees Step in latitude: 0.25 degrees Step in longitude: 0.25 degrees
AUX_WNDCHE	Abdalla2007 wind speed table	data	Sigma0 coverage: [5,19.6] Step in Sigma0: 0.2

2.7.2 Dynamic Auxiliary Data Files

Error! Reference source not found. below provides details of all the dynamic auxiliary data files used in the processing of CryoSat data products. These files have shorter validity periods compared to the static ADFs and variable “start” and “stop” times. Their “start” and “stop” times increase in fixed increments, i.e. daily, weekly, monthly; and appropriate files are selected to cover the processing validity.

The dynamic auxiliary data files are mainly supplied by Système au Sol d'ALTimétrie et d'Orbitographie (SSALTO) - <https://www.aviso.altimetry.fr/es/data/product-information/index.html> They supply:

- the DORIS USO drift correction
- the meteorological files, sourced from Meteo-France via SSALTO, based on data from ECMWF
- the historical pole location files, used to derive the geocentric polar tide
- the solar activity R12 index files, used in the Bent Model Ionospheric corrections
- the daily Global Ionospheric Map (GIM) files
- the daily MOG2D files used for dynamic atmospheric correction

The dynamic sea-ice concentration files are provided by University College London, and are online at <http://cryosat.mssl.ucl.ac.uk/dsic>. These concentrations are derived from the NRT Defense Meteorological Satellite Program (DMSP) Special Sensor Microwave/Imager (SSM/I) data of NSIDC.

Table 7: Dynamic ADFs used in the processing of CryoSat data products

File Type	Description	Provider
AUX_SUNACT	Monthly incremented Solar Activity Index files	SSALTO
AUX_ALTGRD	Gaussian Altimetric Grid used for the computation of all meteo corrections. This is updated only when the horizontal spatial resolution of the ECMWF model is updated	SSALTO
AUX_DORUSO	Daily incremental files of the DORIS USO Drift	SSALTO
AUX_POLLOC	Daily incremental files of the Instantaneous Polar Location	SSALTO
AUX_IONGIM †	Daily dynamic files of the GPS Ionospheric Map	SSALTO

AUX_WETTRP †	Daily dynamic meteo files of Wet Tropospheric Correction *	SSALTO
AUX_U_WIND †	Daily dynamic meteo files of WE Wind component *	SSALTO
AUX_V_WIND †	Daily dynamic meteo files of SN Wind component *	SSALTO
AUX_SURFPS †	Daily dynamic meteo files Surface Pressure *	SSALTO
AUX_SEAMPS †	Daily dynamic meteo files of Mean Ocean Pressure *	SSALTO
AUX_MOG_2D †	Daily dynamic meteo files of Dynamic Atmospheric Correction *	SSALTO
AUX_SEA_IC	Dynamic sea-ice concentration files	UCL/MSSL

† Also available as Forecast ADFs.

A number of Forecast ADFs are used to provide corrections in the FDM products, since the Analysis ADFs are not available at the time of FDM production. These files are computed from forecast model data, and are identified by "AUXI" in the filename.

* Meteo Files.

Meteo files are dynamic ADFs provided on Meteo grids, and use a grid definition file; the Gaussian Altimetric Correction Grid. Each dynamic Meteo grid covers a 6-hour period. Two Meteo grids are required for the computation of a correction: one before and one after the product validity time. These grids are interpolated in time and space in order to derive a correction value for each measurement.

3 CryoSat Data Supply

3.1 CryoSat Ground System

The operational CryoSat Ground System (Payload Data System) is located at the Kiruna receiving station in Sweden. CryoSat data products are distributed by FTP from this site.

3.2 CryoSat User Products

3.2.1 Level 2 Products and Geophysical Data Record

The main CryoSat user products are the L2 products (segmented by measurement mode) and the L2 Geophysical Data Record (GDR; concatenated multi-mode products), which fulfil the needs of most scientific researchers. L2 products contain the time of measurement, the geolocation and the height of the surface above the reference ellipsoid. The surface height is fully corrected for instrument effects, propagation delays, measurement geometry, and other geophysical effects such as atmospheric and tidal effects. The value of each geophysical correction applied to the corrected surface height is provided in the product. The Correction Applied flags (`flag_cor_applied_20_ku`) and Correction Error flags (`flag_cor_err_01`) can be used to determine whether a particular geophysical correction has not been applied, either due to configuration or due to an error.

L2 products also contain mode and quality flagging information, and orbit information. For measurements made in SAR and SIN modes, a freeboard height is computed over sea ice. For measurements made in SIN mode the location includes any across-track offset due to topography (computed from the interferometric phase difference). Measurements are computed along track at intervals of approximately every 300 metres.

GDR products are supplied in full-orbit segments starting and ending at the equator. This means that all the measurements made in each mode, and processed by different chains, are consolidated, in correct time order, and share the same record format. The frequency of consolidated L2 data records is approximately one per second, but each record contains a block of 20 higher-rate (20 Hz) measurements. Consolidated L2 data files are partitioned into whole-orbit segments cut at the ascending equator crossing node (ANX) and therefore each consolidated L2 product is approximately 4948 seconds long.

3.2.2 Freeboard Processing

Following the implementation of freeboard processing at Ice Baseline-C, the L2 SAR products contain freeboard values for records discriminated as sea ice. These values are also present in the corresponding L2 GDR products.

At Ice Baseline-D, freeboard processing was also activated in SIN mode, and freeboard values are provided in L2 SIN products for records discriminated as sea ice.

3.2.3 Slope Correction

In general, over land ice the L2 SIN and LRM data are slope-corrected. The SIN slope correction is calculated from the interferometric phase and the LRM from a slope model. Details are given in [RD 16].

For SIN mode, the longitude and latitude of the echoing point may differ from nadir according to the across-track offset computed from the phase difference. In LRM, they may differ from nadir according to the result of the slope-correction algorithm, where the slope model is used in the processor to determine where the first return came from. The method used for this is similar to

ENVISAT. Please note that, in SIN mode, the DEM is not used to determine where the echo came from. Instead, it is used to provide a flag that states whether the echo may be ambiguous due to phase wrapping.

The DEM used for LRM slope model creation is not the same as the DEM used for SIN ambiguity detection. For the slope model in the LRM processing, the DEMs presented by Helm in [RD 29] are used to create the slope models. The DEM file for Antarctica is available in [RD 30] and for Greenland in [RD 31].

For the ambiguity detection in the SIN mode processing, the 2009 Bamber DEM is used for Antarctica [RD 32] and the 2014 GIMP DEM is used for Greenland [RD 33].

3.2.4 Level 1B Products

CryoSat L1B products are aimed at users who are interested in the SIRAL instrument performance and users who are interested developing their own L2 data processing. These products contain time and geolocation information as well as the SIRAL measurements in engineering units. Calibration corrections are included and have been applied to the window delay computations. Signal propagation delays and other geophysical corrections are included in the product but have not been applied to the range or time delay.

L1B data is segmented according to measurement mode and each mode has a slightly different netCDF format to accommodate the difference in the echoes (different dimension sizes and which parameters are filled or set to fill values).

In pulse-limited (or LRM) mode averaged power echoes are included as for previous altimeter missions. Echoes are 128 samples (or 'bins') long.

In SAR mode the echoes which result from Doppler beam formation are included and consist of 256 samples. There are additional parameters which characterise the distribution of energy across the set of Doppler beams which are directed at a common surface location.

In SIN mode the echoes resulting from the Doppler beam formation process consist of 1024 samples. From the interferometric processing there is also an array of 1024 phase differences, and an array of 1024 coherence terms, computed by comparing the echoes received by both antennas.

Both SAR and SIN products also contain averaged waveforms, but these waveforms are not SAR processed (they are pseudo-LRM or PLRM waveforms).

3.2.5 Near Real Time Products

Near Real Time (NRT) data is derived from the science data stream. It can be used for operational oceanography and meteorology, and to allow monitoring of satellite health and safety beyond the limits of the normal housekeeping telemetry. It is sometimes tailored to specific requirements during calibration and validation campaigns, and details must be obtained on a campaign by campaign basis. (See [RD 2]).

It is expected that NRT products are generated with a latency of 2-3 hours after data acquisition. Previously, NRT products were generated with a latency of > 24 hours, due to the use of and dependency on delivery of the Star Tracker Refined (STR_ATTREF) products, which are only delivered after 24 hours. In order to be able to generate the NRT SAR and SIN products in 2-3 hours after acquisition, it was necessary to separate the NRT chain from the existing Baseline-D IPFs. This allows processing to use the L0 Star Tracker products instead of the Star Tracker ATTREF products without delay.

Please note that while NRT processing should nominally use the DORIS Navigator Orbit (DOR_NAV), occasionally when this is not available in time for processing, the FOS Predicted Orbit (MPL_ORBPRES) is used instead.

3.2.6 Fast Delivery Marine Products

Fast Delivery Marine (FDM) data products are produced from LRM data only, processed as soon as possible after acquisition, typically 2-3 hours. These are due to be decommissioned soon, following the operational delivery of NRT Ocean Products (NOP).

3.3 File Structure

Each CryoSat products is composed of two files:

- XML Header File (.HDR); this consists of a Fixed Header and a Variable Header
- Data Product File: at Baseline-C this is in Earth Explorer Format (.DBL); at Baseline-D this is in NetCDF format (.nc).

For a most users, the data product file will be sufficient to perform scientific use of the data, without the need of the corresponding HDR file. The HDR file is an auxiliary ASCII file which is designed to allow the user to quickly identify the product without looking inside the data file, however it is not mandatory for scientific use of the data.

All of the information provided in the Fixed Header of the HDR file is listed below and most of this is also available in the .nc data files as global attributes:

```
<File_Name> ; <File_Description> ; <Notes>; <Mission> ; <File_Class> ; <File_Type> ;
<Validity_Start> ; <Validity_Stop> ; <File_Version> ; <System> ; <Creator> ; <Creator_Version> ;
<Creation_Date>
```

It should be noted that the global attributes in the .nc data files are named and ordered slightly differently than the HDR file, but the core content of each field is the same.

The Variable Header of the HDR consists of an XML MPH and an XML SPH which have been derived from the corresponding attributes from the data file.

The XML header file has a fixed portion and a variable portion. The fixed portion has the same format in all CryoSat files. The variable portion contains much of the same information as the global attributes in the product file but in XML format.

3.4 File Naming Convention

File names are constructed according to standard guidelines for Earth Explorer missions. All follow the conventional form

```
MM_CCCC_TTTTTTTTTT_yyyymmddThhmmss_YYYYMMDDTHHMMSS_vvvv.ttt
```

where:

MM = the mission identifier, which is CS for CryoSat

CCCC = file class which can be: OFFL (Off-Line Systematic Processing), NRT_ (Near Real Time), TEST (Testing), LTA_ (Long Term Archive)

TTTTTTTTTT= file type as defined in Table 8 below

yyymmddThhmmss = start time window as extracted from Job Order

YYYYMMDDTHHMMSS = stop time window as extracted from Job Order

Cvvv or **Dvvv** = the version number of the file. This can be incremented in the case of reprocessing. “C” corresponds to Baseline-C. “D” corresponds to Baseline-D.

ttt = the extension: **tgz** for a gzipped tar file, **HDR** for an extracted header and **nc** for an extracted NetCDF data file.

Table 8: Relevant File Types

File type	Description
SIR_LRM_1B	SIRAL LRM Level 1B
SIR_FDM_1B	SIRAL FDM Level 1B
SIR_SAR_1B	SIRAL SAR Level 1B
SIR_SIN_1B	SIRAL SIN Level 1B
SIR_LRM_2_	SIRAL LRM Level 2
SIR_FDM_2_	SIRAL FDM Level 2
SIR_SAR_2_	SIRAL SAR Level 2
SIR_SIN_2_	SIRAL SIN Level 2
SIR_SID_2_	SIRAL degraded SIN Level 2
SIR_GDR_2_	SIRAL Geophysical Data Record

This table shows only the file types relevant to the scientific data. Calibration modes and intermediate files (FBR and L2I) are excluded.

The geophysical data records (GDR) meet most scientific needs. A GDR covers a full orbit, starting and ending at the ascending node at the equator, and contains time-ordered records of data from all SIRAL systematic modes (LRM, SAR, and SARIn, so no FDM variant).

3.5 Other Conventions

Background information on all sections below can be found in [RD 10].

3.5.1 Latitude and Longitude Limits

Longitude is expressed from -180 to +180 degrees. Positive east does not contain 180.0, negative west does contain -180.0. This is the same definition as used by Envisat.

3.5.2 Range Correction Sign Convention

The sign convention for all range corrections is that they are added to range.

Since $\text{satellite altitude} - \text{range measurement} = \text{surface height}$

it follows that

$\text{satellite altitude} - (\text{range measurement} + \text{ionospheric correction}) = \text{surface height corrected for the ionosphere effect}$

3.5.3 Timestamp Format

The timestamps in the measurement dataset records are TAI times in seconds past 00:00:00 on 1-JAN-2000.

Note that:

- i) The time in the main and specific product headers is in UTC and not in TAI

ii) Time correlations between UTC and TAI are provided via the orbit files - these must account for the correct offsets due to leap seconds

iii) 1 Jan 2000 at 00:00 UTC = 1 Jan 2000 at 00:32 TAI

See the Hong Kong Time Service website for a detailed discussion of time measurement.
<http://www.hko.gov.hk/wservice/tsheet/timeserv.htm>

3.5.4 Time in L2 GDR Records

In L2 products a record contains a group of up to 20 measurements together with a single set of other parameters. This gives a data rate of approximately one record per second, or 1 Hz, with measurements at approximately 20 Hz. Timestamps for both are provided as above.

Unlike previous missions the instrument telemetry does not create the block of 20 high-rate measurements with the 1 Hz parameters. In the case of CryoSat this is purely a choice within the ground processing system to reduce the L2 data volume. The timestamp for records in the SAR and SIN modes is a function of the Doppler beam processing and not associated with a particular telemetry packet. If a group of 20 measurements spans a measurement mode change (or even 2) then the interval between each of the 20 blocks will not be regular. This would make a consistent definition of a 'middle' time rather difficult. Furthermore, a measurement stream may end at any point within the block of 20. In which case the unused blocks are zero-filled and only serve to pad out the data record. One can only be sure that there is at least one measurement in a record of 20.

For these reasons the 1Hz time is provided corresponding to the first measurement of the 20.

4 References and Acronyms

4.1 Reference Documents

- [RD 1] Angle measurement with a phase monopulse radar altimeter, J.R. Jensen, IEEE Transactions on Antennas and Propagation, Vol 47, No 4, April 1999
- [RD 2] CryoSat-2 Mission and Data Description CS-RP-ESA-SY-0059
- [RD 3] CryoSat: A mission to determine the fluctuations in Earth's land and marine ice fields, Wingham et al, Advances in Space Research, Volume 37, Issue 4, 2006, Pages 841-871
- [RD 4] PDS-SSALTO Interface Control Definitions, CS-ID-ACS-GS-0123
- [RD 5] Specification D'Interfaces Internes SSALTO: Orbitographie Mission SMM-IF-M6-EA-20174-CN
- [RD 6] CryoSat2 Precise Orbit Context CS-TN-ESA-SY-0239
- [RD 7] Earth Explorer Geo Corrections User Manual CS-MA-CLS-GS-0001
- [RD 8] Corrections for altimeter low-level processing at the Earth Observation Data Centre, Cudlip et al, International Journal of Remote Sensing, Volume 15, Issue 4, March 1994, pages 889 - 914
- [RD 9] D.E. Cartwright and A.C. Edden, Corrected tables of tidal harmonics. Geophysical Journal of the Royal Astronomical Society, Volume 33, 1973, pages 253-264
- [RD 10] CryoSat Ice NetCDF L1B Product Format Specification, CS-RS-ACS-ESL-5364
- [RD 11] CryoSat Ice NetCDF L2 Product Format Specification, CS-RS-ACS-ESL-5265
- [RD 12] Sea State Bias in Radar Altimetry Revisited, Hausman and Zlotnicki, Marine Geodesy, 33(S1):336-347, 2010
- [RD 13] SIRAL, a High Spatial Resolution Radar Altimeter for the CryoSat-2 Mission, Rey et al, Geoscience and Remote Sensing Symposium, 2001. IGARSS 2001. IEEE 2001 International, vol 7, pages 3080-3082
- [RD 14] Earth Explorer Mission CFI Orbit Software User Manual, EE-MA-DMS-GS-0004
- [RD 15] Earth Explorer Ground Segment File Format Standards, PE-TN-ESA-GS-0001
- [RD 16] CryoSat-2 L2 Processor Design Summary Document, CS-DD-MSL-GS-2002
- [RD 17] The Mean Echo and Echo Cross Product From a Beamforming Interferometric Altimeter and Their Application to Elevation Measurement, Wingham et al, IEEE Transactions On Geoscience And Remote Sensing, Volume 42, No 10, October 2004, pages 2305-2323
- [RD 18] CryoSat-2 IPF1 Design Summary Document, CS-DD-MSL-GS-0008
- [RD 19] Brown Model Derivatives Walter, Smith, 09 June 2009; revised 19 May 2011.
- [RD 20] E. J. Ferraro and C. T. Swift, "Comparison of retracking algorithms using airborne radar and laser altimeter measurements of the Greenland ice sheet," *Geoscience and Remote Sensing, IEEE Transactions on*, vol. 33, no. 3, pp. 700-707, 1995.
- [RD 21] S. W. Laxon and C. G. Rapley, "Radar altimeter data quality flagging," *Advances in Space Research*, vol. 7, no. 11, pp. 315-318, 1987.
- [RD 22] CryoSat-2 IPF2 Sigma-zero Technical Note, CS-TN-MSL-GS-6005
- [RD 23] Carrère, L. and Lyard, F. (2003). Modeling the barotropic response of the global ocean to atmospheric wind and pressure forcing - comparisons with observations, *Geophys. Res. Lett.*, 30, 1275, doi:10.1029/2002GL016473.
- [RD 24] Lyard, F. et al. (2006). Modelling the Global Ocean Tides: Modern Insights from FES2004. *Ocean Dynamics* 56 : 394-415, doi :10.1007/s10236-006-0086.
- [RD 25] Wunsch, C. (1967). The long-period tides. *Rev. Geophys.* 5 475, doi: 10.1029/RG005i004p00447
- [RD 26] Geophysical Corrections in Level 2 CryoSat Products, IDEAS-VEG-IPF-MEM-1288
- [RD 27] Baseline-C CryoSat Ocean Processor – Ocean Product Handbook, v4.0, <https://earth.esa.int/documents/10174/125272/CryoSat-Baseline-C-Ocean-Product-Handbook>
- [RD 28] Radar altimeter gate tracking: theory and extension", J.R. Jensen, IEEE Transactions on Geoscience and Remote Sensing, Vol 37, No 2, March 1999, section III B

- [RD 29] Helm, V., Humbert, A., and Miller, H.: Elevation and elevation change of Greenland and Antarctica derived from CryoSat-2, *The Cryosphere*, 8, 1539–1559, <https://doi.org/10.5194/tc-8-1539-2014>, 2014.
- [RD 30] Helm, Veit; Humbert, Angelika; Miller, Heinz (2014): Elevation Model of Antarctica derived from CryoSat-2 in the period 2011 to 2013, Links to DEM and uncertainty map as GeoTIFF. <https://doi.org/10.1594/PANGAEA.831392>
- [RD 31] Helm, Veit; Humbert, Angelika; Miller, Heinz (2014): Elevation Model of Greenland derived from CryoSat-2 in the period 2011 to 2013, Links to DEM and uncertainty map as GeoTIFF. <https://doi.org/10.1594/PANGAEA.831393>
- [RD 32] Antarctica: Bamber, Jonathan L., Jose Luis Gomez-Dans, and Jennifer A. Griggs. 2009. Antarctic 1 km Digital Elevation Model (DEM) from Combined ERS-1 Radar and ICESat Laser Satellite Altimetry. Boulder, Colorado USA: National Snow and Ice Data Center. Digital media.
- [RD 33] Greenland: Howat, I.M., A. Negrete, B.E. Smith, 2014, The Greenland Ice Mapping Project (GIMP) land classification and surface elevation datasets *The Cryosphere*, 8, 1509-1518, [doi:10.5194/tc-8-1509-2014](https://doi.org/10.5194/tc-8-1509-2014)

4.2 Acronyms and Abbreviations

AGC	Automatic Gain Control
ANX	Ascending equator crossing Node
API	Application Programming Interface
ASCII	American Standard Code for Information Interchange
CAL 1-4	Calibration modes
CFI	Customer Furnished Item
CLS	Collect Localisation Satellites
CNES	Centre National d'Etudes Spatiales
CoG	Centre of Gravity
CoM	Centre of Mass
COP	CryoSat Ocean Processor
CPOM	Centre for Polar Observation and Monitoring
DAC	Dynamic Atmospheric Correction
DAD	Dynamic Auxiliary Data
DEM	Digital Elevation Model
DMSP	Defense Meteorological Satellite Program
DORIS	Doppler Orbitography and Radiopositioning Integrated by Satellite
DS	Data Set
DSD	Data Set Descriptor
DSR	Data Set Record

DTM	Digital Terrain Model
DTU	Technical University of Denmark
ECMWF	European Centre for Medium-Range Weather Forecasts
EM	Electromagnetic
ESA	European Space Agency
ESL	Expert Support Laboratory
FDM	Fast Delivery Marine
FES	Finite Element Solution
FFT	Fast Fourier Transform
FOS	Flight Operations System
GDR	Geophysical Data Record
GIM	Global Ionospheric Map
GOP	Geophysical Ocean Product
GPS	Global Positioning System
IB	Inverse Barometric correction
IERS	International Earth Rotation Service
IOP	Intermediate Ocean Product
IPFDB	Instrument Processing Facility database
ITRF	International Terrestrial Reference Frame
L1B	Level 1B
L2	Level 2
LRM	Low Rate Mode (synonymous with Pulse Limited Mode)
LTA	Long Term Archive
MDS	Measurement Data Set
MDSR	Measurement Data Set Record
MOG2D	Modèle 2D d'Ondes de Gravité (2D Gravity Waves Model)
MPH	Main Product Header
MSS	Mean Sea Surface
MSSL	Mullard Space Science Laboratory (UCL)
NSIDC	National Snow and Ice Data Center

NOAA	National Oceanic and Atmospheric Administration
NOP	Near Real Time Ocean Product
NRT	Near Real Time
OCOG	Offset Centre of Gravity
ODLE	Ocean Depth / Land Elevation
PCONF	Parameter Configuration File
PDS	Payload Data System
PLRM	Pseudo LRM
POE	Precise Orbit Ephemeris
RMS	Root Mean Squared
Rx	Receive (electronics or antenna)
SAD	Static Auxiliary Data
SAR	Synthetic Aperture Radar
SARIn	SAR Interferometry mode
SIN	SAR Interferometry mode
SID	SIN degraded mode
SIRAL	Synthetic Aperture Interferometric Radar Altimeter
SPH	Specific Product Header
SS	Space Segment
SSALTO	Système au Sol d'ALTimétrie et d'Orbitographie
SSB	Sea State Bias
SSHA	Sea Surface Height Anomaly
SSM/I	Special Sensor Microwave/Imager
SWH	Significant Wave Height
TAI	International Atomic Time (from the French, Temps Atomique International)
T/P	TOPEX/Poseidon
Tx	Transmit (electronics or antenna)
UCL	University College London
USO	Ultra-Stable Oscillator
UTC	Coordinated Universal Time

XML Extensible Markup Language